

PREPARATION AND PROPERTIES OF ORGANIC ELECTROLYTES

PREPARATION AND PROPERTIES
OF ORGANIC ELECTROLYTES
FOR ELECTROCHEMICAL DEVICES

電気化学デバイス用有機電解質の合成と性質

宇 恵 誠

①

**PREPARATION AND PROPERTIES
OF ORGANIC ELECTROLYTES
FOR ELECTROCHEMICAL DEVICES**

by

Makoto Ue

Mitsubishi Petrochemical Co. Ltd.,
Tsukuba Research Center,
8-3-1 Chuo Ami Inashiki
Ibaraki 300-03, JAPAN.

Submitted to The University of Tokyo

1994

Preface

This paper is the thesis for a doctorate in engineering of The University of Tokyo.

Rapid growth in electronic industries has given to the author an opportunity to study in the interdisciplinary area between synthetic chemistry and electrochemistry. The author was basically a synthetic chemist, who was highly disciplined by Professor Masanobu Hidai and Emeritus Professor Yasuzo Uchida, and acquired his master's degree from The University of Tokyo in 1981. After three years' experience as a synthetic chemist in the MITI's "C1" national project at Mitsubishi Petrochemical Co., the author has solely jumped into the research of organic electrolytes for electronic devices in 1984, which was an unknown area for most chemical companies. The author has succeeded in finding an epoch-making organic electrolyte based on a quaternary ammonium carboxylate salt and γ -butyrolactone in 1985, which is now supplied to almost all manufactures of aluminum electrolytic capacitors in the world. The author has also succeeded in finding a new cyclic quaternary ammonium tetrafluoroborate salt in 1986, which is partly used as a supporting electrolyte salt for electrical double layer capacitors. After that the author had an opportunity to study electrochemistry in the United States from 1988 to 1990. The studies both at University of Pittsburgh and Lawrence Berkeley Laboratory (operated by University of California at Berkeley for the US Department of Energy) were oriented to the lithium batteries, whose electrolytes are also manufactured by our company.

The content of this paper, which encompasses the preparation and properties of organic electrolytes for aluminum electrolytic capacitors, electrical double layer capacitors and lithium batteries, including the industrialized materials in Mitsubishi Petrochemical Co., provides a good successful example of the research and development, because the electrolyte business is no more a niche field due to the advent of the rechargeable lithium ion battery, which is regarded as one of the strategic products for many portable electronic appliances.

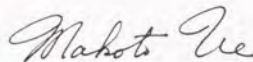
In the first chapter, some electrochemical devices using organic electrolytes are introduced and several fundamental requirements for these organic electrolytes are presented. In addition, the basic properties of organic solvents and the importance of purification are briefly explained. On the basis of the above knowledge, chapters 2, 3 and 4 are devoted to the research results on the organic electrolytes for aluminum electrolytic capacitors, electrical double layer capacitors and lithium batteries, respectively. Chapter 5 contains solid organic electrolytes. Organic electrolytes containing a new gelling agent are proposed as a quasi-solid electrolyte for a thin film rechargeable lithium cell. Application of the polymer electrolytes for a thin film rechargeable lithium cell using organodisulfide and titanium disulfide cathodes is also given. In chapter 6, electrical conductance theories and a computer program are given, on which the conductometric analysis of the dilute solutions of organic electrolytes is carried out. In the last chapter, the papers, society meeting abstracts and patents are listed, on which this thesis is based.

I wish to express my sincere appreciation to Mitsubishi Petrochemical Co., who is about to be reborn, and Professor M. Hidai in The University of Tokyo, who give me an opportunity to get a doctorate.

I wish to thank many of my colleagues worked together in Mitsubishi, among them Mr. Tadashi Ayusawa, Dr. Shoichiro Mori, Mr. Naohiro Nojiri, Mr. Makoto Imanari, Mr. Katsuo Hyuga, Mr. Toshiaki Miyagawa, Mr. Takayuki Kawahara, Mr. Hitoshi Asahina, Mr. Eiki Yasukawa, Mr. Mitsumasa Kaitoh, Mr. Katsuaki Hasegawa, Mr. Kazuhiko Ida, Ms. Asao Kominato, Mr. Kunihisu Shima, Mr. Tomohiro Sato, Mr. Masayuki Takeda and Ms. Sachie Sekigawa.

I am also grateful to Emeritus Professor Johannes F. Coetzee (Department of Chemistry, University of Pittsburgh), who took me to the world of solution chemistry, and Professor Lutgard C. De Jonghe (Department of Materials Science and Mineral Engineering, University of California at Berkeley), who gave me an opportunity to study the ECSJ-Award winning theme. Many thanks to Dr. Balasaheb. K. Deshmukh (Analytical Sciences, Dow Chemical Co.), Dr. Steven J. Visco (Materials Sciences Division, Lawrence Berkeley Laboratory), Professor Michael M. Lerner (Department of Chemistry and Center for Advanced Materials Research, Oregon State University) and Professor Meilin Liu (School of Materials Science and Engineering, Georgia Institute of Technology) for their valuable discussions.

The writing of papers and this thesis has been a labor of love and pain aided by the support of my family. I wish to thank my wife, Akemi, and four children, Nozomi, Tsubasa, Aoi and Akane for their patience.



Makoto Ue
Senior Research Chemist
Tsukuba Research Center
Mitsubishi Petrochemical Co.

Ami, Ibaraki
August 25, 1994

Contents

| | |
|----------------------------------------------------------------|-----|
| 1. An Overview | 1 |
| 1.1. Introduction | 1 |
| 1.2. Requirements for Organic Electrolytes | 2 |
| 1.3. General Features of Organic Solvents | 4 |
| 1.4. Importance of Purification | 6 |
| 1.5. Summary | 7 |
| 1.6. General References | 8 |
| 2. Organic Electrolytes for Aluminum Electrolytic Capacitors | 9 |
| 2.1. Introduction | 9 |
| 2.2. Preparation of Electrolyte Salts | 13 |
| 2.3. Electrochemical Properties of Organic Electrolytes | 14 |
| 2.4. Conductometric Analysis of Quaternary Ammonium Salts | 20 |
| 2.5. Conductometric Analysis of Tertiary Ammonium Salts | 28 |
| 2.6. Anodic Oxidation of Aluminum in Organic Electrolytes | 32 |
| 2.7. Characterization of Aluminum Anodic Oxide Films | 45 |
| 2.8. Chemical Stability of Organic Electrolytes | 54 |
| 2.9. Organo-Boron Complexes | 58 |
| 2.10. Summary | 67 |
| 2.11. References | 68 |
| 3. Organic Electrolytes for Electrical Double Layer Capacitors | 71 |
| 3.1. Introduction | 71 |
| 3.2. Preparation of Electrolyte Salts | 73 |
| 3.3. Electrochemical Properties of Organic Electrolytes | 75 |
| 3.4. Conductometric Analysis of Diluted Solutions | 88 |
| 3.5. Summary | 94 |
| 3.6. References | 95 |
| 4. Organic Electrolytes for Lithium Batteries | 98 |
| 4.1. Introduction | 98 |
| 4.2. Electrochemical Properties of Organic Electrolytes | 101 |
| 4.3. Conductometric Analysis of Diluted Solutions (1) | 104 |
| 4.4. Conductometric Analysis of Diluted Solutions (2) | 115 |
| 4.5. Correlation between Concentrated and Diluted Solutions | 123 |
| 4.6. Summary | 125 |
| 4.7. References | 126 |

| | |
|--------------------------------------------------------------|-----|
| 5. Solid Organic Electrolytes for Rechargeable Lithium Cells | 129 |
| 5.1. Introduction | 129 |
| 5.2. Quasi-Solid Organic Electrolytes | 130 |
| 5.3. Solid Polymer Electrolytes | 135 |
| 5.4. Summary | 146 |
| 5.5. References | 147 |
| 6. Appendixes | 149 |
| 6.1. Electrical Conductance Theory | 149 |
| 6.2. Examples of Conductivity Fitting | 154 |
| 6.3. Program for Conductivity Analysis | 155 |
| 6.4. References | 172 |
| 7. Conclusions | 173 |
| 8. List of Publications | 174 |
| 8.1. Papers | 174 |
| 8.2. Society Meetings | 177 |
| 8.3. Patents | 180 |

1. An Overview

1.1. Introduction

Recent rapid growth of microelectronics has spread its influence on every industry. Demand for lightweight, compact electronic equipment in both consumer and industrial applications has been requesting lighter, thinner, shorter and smaller electronic components. This trend becomes stronger and stronger, when portability is the prime requisite for the electronic appliances such as laptop personal computers, camcorders and cellular phones.

Among the electronic components, there are several electrochemical devices, where an organic electrolyte is one of the key materials that determine the electrical properties of the devices. Typical examples of these electrochemical devices are shown in Table 1, where main compositional materials are listed.

An aluminum electrolytic capacitor is the most important electrochemical device from the viewpoint of annual output (205 billion Japanese yen in 1991) as shown in Table 2. The second one is a lithium battery, whose output is only 50 billion Japanese yen, however, it is expected to increase rapidly due to the popularization of secondary (rechargeable) lithium batteries. Third one is an electrical double layer capacitor, which is an intermediate device between capacitor and battery. The last one is an electrochromic display, which failed in competition with a liquid crystal display and now is waiting commercialization as a smart window.

Table 1. Typical examples of electrochemical devices using organic electrolytes.

| Device | Anode | Electrolyte | Cathode |
|-----------------------------------|--------------------|---------------------------------------------------------------------------------------------------|---------|
| Aluminum electrolytic capacitor | Al_2O_3 |  Me_4N /GBL | Al |
| Lithium battery | Li | $LiClO_4/PC+DME$ | MnO_2 |
| Electrical double layer capacitor | C | Et_4NBF_4/PC | C |
| Electrochromic display | $Fe_4[Fe(CN)_6]_3$ | $LiClO_4/PC$ | WO_3 |

GBL; γ -butyrolactone, PC; propylene carbonate, DME; dimethoxyethane.

Table 2. Annual output of electrochemical devices in 1991.

| Device | Quantity (million pcs.) | Value (billion yen) |
|-----------------------------------|-------------------------|---------------------|
| Aluminum electrolytic capacitor | 26442 | 205.4 |
| Lithium battery (primary) | 376 | 48.5 |
| Lithium battery (secondary) | 10 | 2.1 |
| Electrical double layer capacitor | 122 | 6.3 |

1.2. Requirements for Organic Electrolytes

The reason the organic electrolyte *i.e.* nonaqueous electrolyte is preferred is that the assortment of solvents with widely varying properties, almost unlimited number of solvent mixtures and solute compounds provides flexibility in tackling a given problem.

Although the chemicals used for the organic electrolytes vary considerably in each device, there are several fundamental requirements common to all these electrolytes.

These requirements are as follows:

- 1) *High chemical stability*
- 2) *Wide operational temperature range*
- 3) *High electrolytic conductivity*
- 4) *Good compatibility with electrodes*
- 5) *High safety*
- 6) *Low cost*

A wide liquid range (requirement 1, 2) and a wide accessible potential range (electrochemical window, a part of requirement 4) are main factors that recommend nonaqueous electrolytes rather than aqueous electrolytes for use in the electrochemical devices.

For example, the operational temperature for a popular aluminum electrolytic capacitor ranges from -55°C to 105°C and the nominal voltage for a single lithium cell is 3 V, which cannot be realized by any aqueous electrolytes due to the high melting point, low boiling point and narrow electrochemical window of water, itself.

Drawbacks of nonaqueous electrolytes include lower electrolytic conductivities (requirement 3), when compared to aqueous electrolytes or molten salts as indicated in Table 3, where the electrolytic conductivities of several technically important ionic conductors are compared [1]. Other disadvantages arise from the toxicity or flammability of the electrolyte materials (requirement 1, 5) and their appreciably higher costs (requirement 6). The compatibility with electrodes (requirement 4) includes complex chemistry, which depends on the nature of the device and of course, the kind of the electrode. This requirement will be explained in detail in each chapter.

Table 3. Electrolytic conductivities of several technically important ionic conductors.

| System | | Temp. / °C | Conductivity / mS cm ⁻¹ |
|-------------|------------------------------------------------------------------------------------------------------|------------|------------------------------------|
| Aqueous | *5.68 M HCl/H ₂ O | + 25 | 849 |
| | *6.80 M | - 20 | 353 |
| | 2.81 M LiClO ₄ /H ₂ O | + 25 | 152 |
| | 2.84 M | 0 | 88 |
| Nonaqueous | *0.66 M LiClO ₄ /PC | + 25 | 5.4 |
| | *0.34 M | - 45 | 0.3 |
| | *1.39 M LiClO ₄ /PC(42wt%)+DME | + 25 | 14.6 |
| | *0.74 M LiClO ₄ /PC(28wt%)+DME | - 45 | 3.3 |
| Molten salt | LiCl | + 637 | 5854 |
| | Me-N ⁺ (O ⁻)N ⁻ -Et AlCl ₄ | + 25 | 20.6 |
| Solid | Li ₃ N | + 25 | 1 |
| | Li(CF ₃ SO ₂) ₂ N/(CH ₂ CH ₂ O) _n | + 25 | 0.1 |

* the concentration where maximum conductivity was obtained.

1.3. General Features of Organic Solvents

An organic electrolyte is basically composed from a solvent and a solute. Although the properties of the organic electrolyte are dependent on both the solvent and the solute, it is desirable to describe the solvent properties before moving to special topics.

Two aspects determine the role of solvent. One is the bulk properties of the solvent, *i.e.* relative permittivity ϵ_r , viscosity η and density d , the other is the electron donor or acceptor abilities of the solvent (DN; donar number, AN; acceptor number). Various attempts have been made to classify solvents on the basis of various criteria, however, classification on the basis of the acid-base properties and the magnitude of relative permittivity seems to be rational (*cf.* Fig. 1). A typical modern breakdown differentiates between the following types of solvents: "amphiprotic" (sometimes called simply "protic"), which means capable of accepting and donating protons and "aprotic", which means incapable of transferring protons to any appreciable extent. Aprotic solvents can be divided into two categories. "Dipolar aprotic" solvents are moderately good solvating and ionizing media due to their dipolar nature and their intermediate relative permittivity. Within the dipolar aprotic class Kolthoff makes a further fine distinction between solvents that are protophilic (slightly basic) and protophobic (without basic properties). "Inert" solvents are nonpolar aprotic liquids characterized by low relative permittivity ($\epsilon_r < 10$).

It is the dipolar aprotic solvent that is important for electrochemical devices, because it gives distinctly different electrochemical properties from water. The physicochemical properties of some dipolar aprotic solvents are given in Table 4, where protophilic ones are signed with asterisk.

Table 4. Physical properties of dipolar aprotic solvents at 25°C.

| Solvent | ϵ_r /- | mp /°C | bp /°C | η / cp | d / g cm ⁻³ | DN | AN |
|-------------------------------|----------------------------------|-----------|-----------|-------------------|-----------------------------|------|------|
| Ethylene carbonate (EC) | ^{340°C} 90 ^a | 37 | 238 | 1.85 ^a | 1.32 | 16.4 | |
| Propylene carbonate (PC) | 65 | -49 | 242 | 2.51 | 1.20 | 15.1 | 18.3 |
| Dimethylsulfoxide (DMSO) * | 47 | 19 | 189 | 1.99 | 1.10 | 29.8 | 19.3 |
| Sulfolane (TMS) | ^{30°C} 43 ^b | 28 | 287 | 10.0 ^b | 1.26 | 14.8 | 19.2 |
| γ -Butyrolactone (GBL) | 42 | -44 | 204 | 1.73 | 1.12 | 18 | |
| Nitromethane (NM) | 38 | -29 | 101 | 0.62 | 1.13 | 2.7 | 20.5 |
| Dimethylformamide (DMF) * | 37 | -61 | 153 | 0.80 | 0.94 | 26.6 | 16.0 |
| Acetonitrile (AN) | 36 | -49 | 82 | 0.34 | 0.78 | 14.1 | 18.9 |
| Methyl formate (MF) | 9 | -99 | 32 | 0.33 | 0.97 | | |
| 1, 2-Dimethoxyethane (DME) * | 7 | -58 | 85 | 0.41 | 0.86 | 20 | 10.2 |
| Tetrahydrofuran (THF) * | 7 | -109 | 66 | 0.46 | 0.88 | 20 | 8.0 |
| 1, 3-Dioxolane (DO) * | 7 | -95 | 78 | 0.59 | 1.06 | | |
| Dimethyl carbonate (DMC) | 3 | 3 | 90 | 0.59 | 1.06 | | |

?
 1. Acid-base properties (pK_s) 30
 2. Relative permittivity (ϵ_r) 20

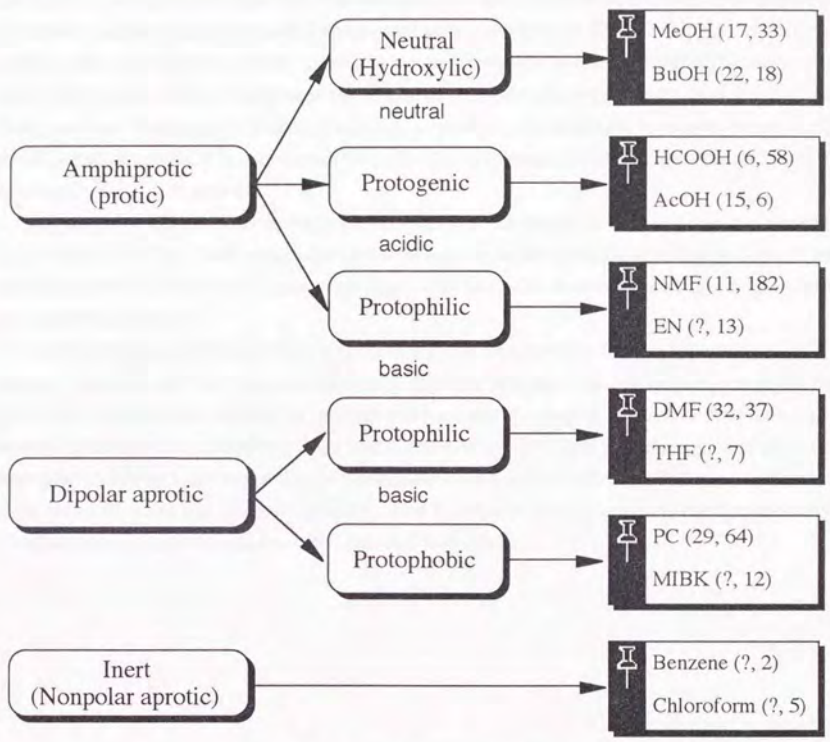
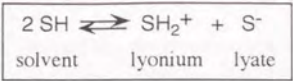


Fig. 1. Classification of solvent

1.4. Importance of Purification

In aprotic solvent systems useful for electrochemical device applications, the presence of even trace impurities in the electrolyte can affect the performance and reliability of the system. For example, a few ppm of chloride ion corrode aluminum electrodes in the aluminum electrolytic capacitors, a few ppm bromide ion deteriorate the performance of electrical double layer capacitors operated at an elevated temperature, and several tens ppm of water degrade lithium anode in the lithium cells. It is very important, therefore, to use thoroughly purified materials. No solvent or solute can be said to have been adequately explored unless they have been very carefully purified. Since many of the organic solvents of interest are made by condensation reactions, which are to some extent reversible, it is common to find other protic substances like alcohols, organic acids as potentially harmful impurities.

The author would like to mention that much time was consumed for the purification of solvents and solutes rather than their preparation, even though the troublesome purification procedures are omitted in this thesis. In some cases, a synthetic route had to be altered to avoid the contamination of a harmful impurity.

Purification procedures vary from solvent to solvent, depending on its properties, including thermal stability, and the type and amount of impurity present. The purification strategies for individual solvents are outlined in several publications. Generally, fractional distillation and recrystallization were effective for the purification of solvents and solutes, respectively. It is important to identify the impurities both qualitatively and quantitatively. The most commonly used methods were gas chromatography, liquid chromatography and ion chromatography. Voltammetry and conductometry were also used very often.

1.5. Summary

In this first chapter, some electrochemical devices using organic electrolytes were introduced and several fundamental requirements for these organic electrolytes were presented. In addition, the basic properties of organic solvents were explained and it was shown that the dipolar aprotic solvent is important for electrochemical devices, because it gives distinctly different electrochemical properties from water. The physicochemical properties of some dipolar aprotic solvents and the importance of purification were briefly explained.

There are many books that deal with fundamentals of nonaqueous solution chemistry. These are listed in the next section.

1.6. General References

Main books in this field published after 1970 were listed here.

1. J. Barthel, H. J. Gores, G. Schmeer and R. Wachter, "Non-Aqueous Electrolyte Solutions in Chemistry and Modern Technology", *Topics in Current Chemistry*, **111**, 33 (1983).
2. J. F. Coetzee, Editor, *Recommended Methods for Purification of Solvents and Tests for Impurities*, Pergamon Press, Oxford (1982).
3. O. Popovych and R. P. T. Tomkins, *Nonaqueous Solution Chemistry*, Wiley-Interscience, New York (1981).
4. I. M. Kolthoff and P. J. Elving, Editors, *Treatise on Analytical Chemistry*, Wiley-Interscience, New York, Vol. I (1978), Vol. II (1979).
5. V. Gutmann, *The Donor-Acceptor Approach to Molecular Interactions*, Plenum Press, New York (1978).
6. J. E. Gordon, *The Organic Chemistry of Electrolyte Solutions*, Wiley, New York (1975).
7. A. K. Convington and T. Dickinson, Editors, *Physical Chemistry of Organic Solvent Systems*, Plenum Press, London (1973).
8. G. J. Janz and R. P. T. Tomkins, Editors, *Nonaqueous Electrolyte Handbook*, Academic Press, New York, Vol. I (1972), Vol. II (1973).
9. J. C. Marchon, Editor, *Non Aqueous Electrochemistry*, Butterworths, London (1971).
10. J. A. Riddick and W. B. Bunger, *Organic Solvents*, 3rd ed., Wiley-Interscience, New York (1970).
11. J. F. Coetzee and C. D. Ritchie, Editors, *Solute-Solvent Interactions*, Marcel Dekker, New York, Vol. I (1969), Vol. II (1976).
12. J. J. Lagowski, Editor, *The Chemistry of Non-aqueous Solvents*, Academic Press, New York, Vol. I-V (1966-1978).
13. R. A. Robinson and R. H. Stokes, *Electrolyte Solutions*, 2nd ed. rev., Butterworths, London (1970).

2. Organic Electrolytes for Aluminum Electrolytic Capacitors

2.1. Introduction

An aluminum electrolytic capacitor contains an aluminum oxide dielectric, which is formed by the anodic oxidation of an aluminum foil electrode. This capacitor had achieved an important position in circuit applications through its unsurpassed volumetric efficiency of capacitance and low cost per unit of capacitance by 1952 [1]. Electric charges Q stored in the dielectric are determined by CV product, where C and V are capacitance and applied voltage, respectively. The large capacitance of the aluminum electrolytic capacitor is achieved by the presence of an extremely thin dielectric oxide film on aluminum anode ($< 1 \mu\text{m}$) and by the creation of a high surface area of the anode foil through electrochemical etching (roughness factor > 100). An organic electrolyte is used as a true cathode, which enables to penetrate into the fine porous structure and to obtain the largest possible capacitance as shown in Fig. 1. The appearance and construction of the capacitor are given in Fig. 2. The production process is depicted in Fig. 3. Attention must be paid to the fact that there are two different electrolytes for the production of the aluminum electrolytic capacitors. One is a "forming electrolyte" and the other is an "operating electrolyte". The former is the aqueous electrolyte used in the production of the anodized aluminum foil, and the latter is the nonaqueous electrolyte used inside the capacitor.

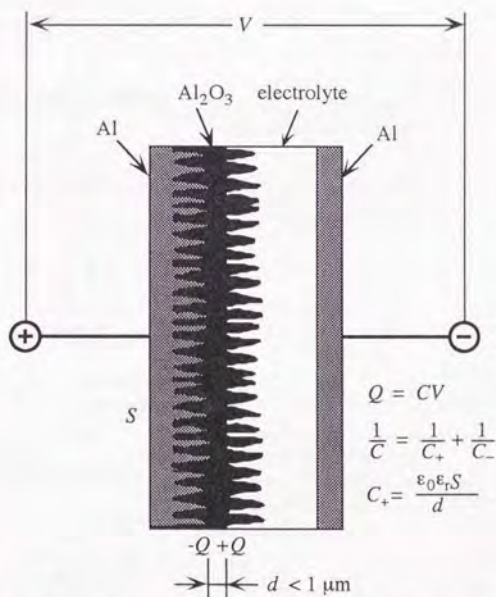


Fig. 1. Principle of aluminum electrolytic capacitor.

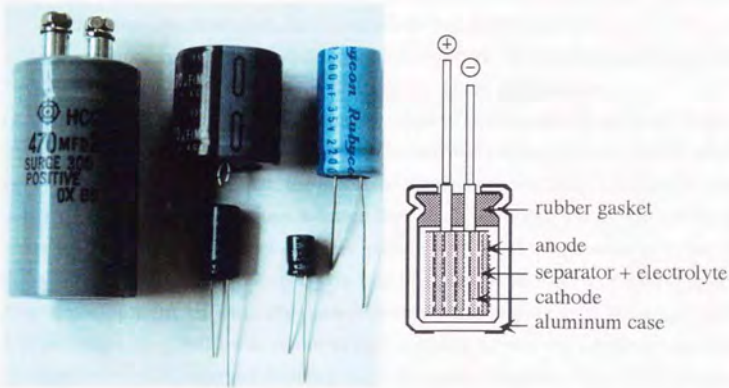


Fig. 2. Appearance and construction of aluminum electrolytic capacitors.

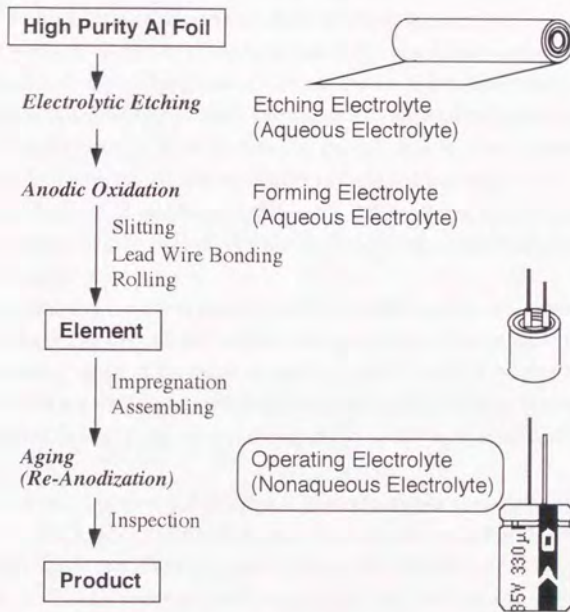


Fig. 3. Production process of aluminum electrolytic capacitors.

Advances of great significance have been made through the research and development on its two principal components; the foil electrode and the operating electrolyte. This progress has been demonstrated by a marked reduction in size, extension of the operating temperature range, improved electrical characteristics, increased reliability, and longer life.

The information on the organic electrolytes for aluminum electrolytic capacitors is very limited [1 - 3], however, many formulations are disclosed in patent applications.

In the early 1950's virtually all aluminum electrolytic capacitors utilized as the operating electrolyte the reaction mixture of ammonium borate and ethylene glycol, which was developed twenty years earlier [1]. However, the increased demands of electronic equipment manufacturers for more rigorous service conditions revealed that the glycol-borate electrolyte system had serious limitations. High melting point of ethylene glycol (-13°C) and the presence of water arisen from the esterification reaction between two principal components restrict its operation to -25 - 85°C.

The development of entirely new electrolyte systems has been carried out and dimethylformamide (DMF) was found to be a suitable solvent for capacitor application. The DMF-based electrolyte enlarged the operation temperature range to -55 - 125°C, although special chemically resistant closures such as a Teflon seal with a butyl rubber gasket were required. In addition to DMF, a number of other organic solvents have found application, particularly, γ -butyrolactone (GBL) became a major solvent.

Concurrent with the introduction of new solvents, the development of an extensive number of solutes has been carried out. Organic compounds dominated this field and the salts of carboxylic acids such as adipic acid, maleic acid and salicylic acid, found application.

Although the particular choice of electrolyte among this bewildering array of possibilities is determined by many factors, the emergence of many alternative systems permitted capacitors to be more closely tailored to diverse applications. The author has classified the organic electrolytes into four categories from the historical view as shown in Table 1. It is the fourth generation which the author has found. For more details, refer to author's reviews and patents [4-7].

The electrolytic conductivity and the electrochemical stability of the organic electrolyte are the major controlling factors to determine the dissipation factor (internal resistance) and the shelf life of the capacitor, respectively.

A specific compatibility condition must be fulfilled for the organic electrolyte of aluminum electrolytic capacitors. The electrolyte should act as a good oxide forming agent, maintaining the electrochemical state of repair of the oxide layer during the life time of the capacitor. Since the edge parts of the capacitor element must be anodized in the operating electrolyte during the aging process as illustrated in Fig. 3, this film forming ability is the very important property of the electrolyte.

When aluminum metal is anodically oxidized in an electrolyte containing water, aluminum oxide is produced in the form of a film on the metal surface as shown in Fig. 4. Depending on the type of electrolyte used, two distinct types of layers are formed, whose characteristics are compared in Fig. 5. The barrier-type oxide characterized by low porosity and high resistivity represents the basis of aluminum electrolytic capacitor production.

Table 1. Typical examples of organic electrolytes for aluminum electrolytic capacitors.

| Generation | Solvent | Acid component | Base component |
|------------|----------|----------------|---------------------|
| 1st | GLY, EG | Boric acid | Ammonia |
| 2nd | EG | Adipic acid | Ammonia |
| 3rd | DMF, GBL | Maleic acid | Triethylamine |
| 4th | GBL | Phthalic acid | Tetramethylammonium |

GLY; glycerine, EG; ethylene glycol, DMF; N,N-dimethylformamide, GBL; γ -Butyrolactone.

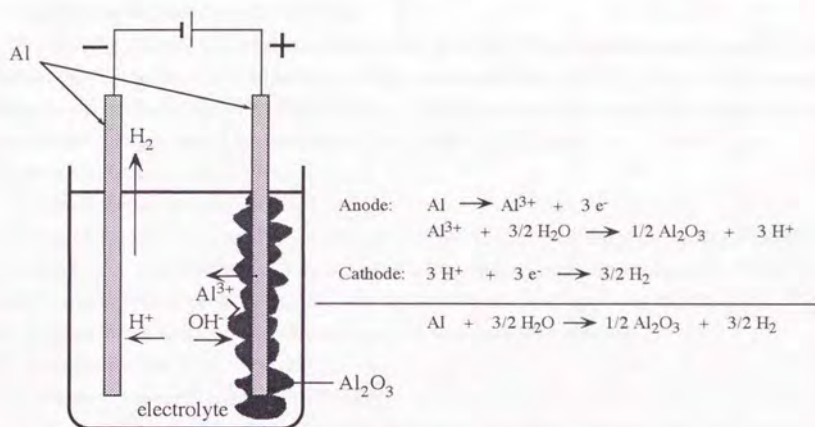


Fig. 4. Principle of anodic oxidation of aluminum.

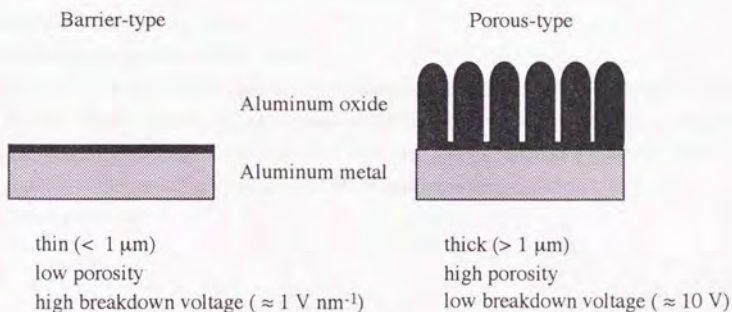


Fig. 5. Comparison between barrier and porous-type anodic oxide films.

2.2. Preparation of Electrolyte Salts

Quaternary ammonium carboxylates were prepared by the neutralization of carboxylic acids with quaternary ammonium aqueous alkali solutions.

1) Tetraethylammonium salts were prepared by the titration of carboxylic acids with tetraethylammonium hydroxide aqueous solution (SACHEM Inc.). <Method A>

2) Tetramethyl-, ethyltrimethyl-, diethyldimethyl- and triethylmethylammonium carboxylates were prepared by the neutralization of carboxylic acids with the corresponding quaternary ammonium bicarbonate aqueous solutions obtained from the reaction of appropriate amines with dimethyl carbonate. <Method B> For more details, refer to author's patent [8].

All salts were recrystallized from acetone and then vacuum dried.

2.2.1. Experimental

Preparation of quaternary ammonium bicarbonate aqueous solutions are described below.

Tetramethylammonium methylcarbonate

67.5 g (0.75 mol) of dimethyl carbonate, 36.9 g (0.62 mol) of trimethylamine and 90 g of methanol were filled in a 300 ml autoclave. They were reacted at 110°C for 3 hours. The reaction pressure was about 6 kg cm⁻². The unreacted materials and the solvent were removed by evaporation. The amount of the resulting solid was 85.0 g (0.57 mol).

The yield was 92.5 %. mp: 127°C.

Tetramethylammonium bicarbonate

53.2 g (0.36 mol) of tetramethylammonium methylcarbonate was dissolved in 53.2 g of water in a 300 ml three neck distillation flask equipped with a thermometer and a condenser. While the mixture was refluxed at 40°C and 20 mmHg for 1 hour, methanol was distilled off. The concentration of the resulting aqueous solution was determined by titration.

The yield was 95.0 %. mp: 75°C (solid).

Triethylmethylammonium methylcarbonate

117.2 g (1.30 mol) of dimethyl carbonate, 101.2 g (1.00 mol) of triethylamine and 101.2 g of methanol were filled in a 500 ml autoclave. They were reacted at 120°C for 14 hours. The average reaction pressure was about 6 kg cm⁻². The unreacted materials and the solvent were removed by evaporation. The amount of the resulting solid was 180.0 g (0.94 mol).

The yield was 94.1 %. mp: 46°C.

Triethylmethylammonium bicarbonate

150.0 g (0.69 mol) of triethylmethylammonium methylcarbonate was dissolved in 150.0 g of water in a 500 ml three neck distillation flask equipped with a thermometer and a condenser. While the mixture was refluxed at 40°C and 20 mmHg for 1 hour, methanol was distilled off. The concentration of the resulting aqueous solution was determined by titration.

The yield was 95.0 %.

2.3. Electrochemical Properties of Organic Electrolytes

Carboxylic acids and their salts have been tested as a solute for both operating electrolyte and forming electrolyte. These include formic acid, acetic acid, propionic acid, butyric acid, oxalic acid, malonic acid, succinic acid, adipic acid, maleic acid, salicylic acid, phthalic acid, lactic acid, citric acid and tartaric acid [9 - 11]. However, most work was carried out in aqueous solutions and there is no systematic data in nonaqueous solutions.

Therefore, the author examined the electrolytic conductivity and scintillation voltage of organic electrolytes based on these carboxylic acids.

2.3.1. Experimental

Electrolyte preparation

Formic acid, acetic acid, caproic acid and oxalic acid were used as received. Adipic acid, maleic acid, benzoic acid, salicylic acid and phthalic acid were purified by recrystallization from water.

Neutral ammonium salts were prepared by the titration of the carboxylic acids with 25% aqueous ammonia (Nakalai Tesque, Inc.), followed by recrystallization and vacuum drying. These ammonium salts were dissolved in ethylene glycol (Wako Pure Chemical Industries).

Neutral amine salts were prepared *in situ* by the neutralization of carboxylic acids with triethylamine (Wako Pure Chemical Industries) in γ -butyrolactone (Mitsubishi Petrochemical Co.).

Triethylmethylammonium hydrogen maleate (TEMAM), tetramethylammonium hydrogen phthalate (TMAP) were prepared by the neutralization of the acids with the corresponding quaternary ammonium bicarbonate aqueous solutions (See Chap. 2.2). These were dissolved in γ -butyrolactone and the resulting electrolytes were vacuum dried.

Measurements

The electrolytic conductivity and water content of electrolytes were measured by a conductivity meter equipped with a standard type conductivity cell (Toa Electronics, CM-30S/CGT-511B) and a moisture meter (Mitsubishi Kasei Co., CA-06), respectively.

The scintillation voltage was measured by the galvanostatic anodization of aluminum. A smooth aluminum foil of 100 μm thickness and 99.99 % purity (Mitsubishi Aluminum Co.) was cut into a 10 x 20 mm rectangle with a thin long tag for electrical contact. This flag shape coupon was washed with acetone and pure water, followed by drying in air. A constant current of 0.5 A dm^{-2} was applied to this coupon in an organic electrolyte from a power source (Kikusui Electronics Co., PAD500-2L), and the voltage across the cell was recorded on an intelligent recorder (Toa Electronics, INR-6061).

2.3.2. Results and Discussion

Traditional electrolytes

The salts of carboxylic acids were evaluated in both ethylene glycol (EG) and γ -butyrolactone (GBL). Since most ammonium carboxylate salts did not dissolve in GBL, triethylammonium salts were used for GBL electrolytes. The electrolytic conductivity σ at 25°C and scintillation voltage V_s at 0.5 A dm⁻² of 10 wt % solution are given in Table 2.

The salts of smaller and/or stronger acid generally showed higher electrolytic conductivity with lower scintillation voltage. Scintillation was not observed for monocarboxylic acids, and therefore, the maximum voltage attained was given in parenthesis. This is the indication of inferior film forming ability of monocarboxylic acids [9].

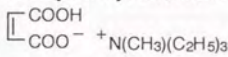
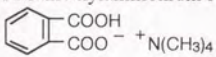
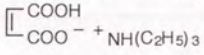
Table 2. Electrolytic conductivity and scintillation voltage of organic electrolytes.

| Carboxylic Acid | <i>pKa</i> | <i>MW</i> | EG-NH ₄ system | | GBL-NEt ₃ system | |
|-----------------|------------|-----------|-----------------------------------|--------------|-----------------------------|-------|
| | | | σ / mS cm ⁻¹ | V_s / V | σ | V_s |
| Formic acid | 3.75 | 46.0 | 7.5 | (46) | 4.0 | (123) |
| Acetic acid | 4.76 | 60.1 | 4.6 | (90) | 0.8 | (120) |
| Caproic acid | 4.88 | 116.2 | 1.3 | (524) | 0.6 | (467) |
| Oxalic acid | 1.27 | 90.0 | insoluble | | 1.4 | 180 |
| Adipic acid | 4.43 | 146.1 | 3.2 | 376 | 0.6 | 448 |
| Maleic acid | 1.94 | 116.1 | 4.0 | 175 | 2.8 | 133 |
| Benzoic acid | 4.21 | 122.1 | 2.7 | 390 | 0.8 | 333 |
| Salicylic acid | 3.00 | 138.1 | 2.9 | 186 | 1.2 | 162 |
| Phthalic acid | 2.95 | 166.1 | 2.2 | 147 | 1.8 | 130 |

New electrolytes

During the course of pursuing a highly conductive electrolyte, the author has found that quaternary ammonium salts of carboxylic acids show much higher conductivities than tertiary ammonium counterparts in γ -butyrolactone. Outstanding electrochemical properties of the quaternary ammonium carboxylate/ γ -butyrolactone electrolytes will be demonstrated in comparison with the traditional electrolytes. The chemical structures and abbreviations of the used solutes are given in Table 3.

Table 3. Chemical structures and abbreviations of the solutes used.

| | |
|--------------------------|----------------------------------------------------------------------------------------------------------------------------------------------------------------------------------------------------------------------------------------------------------------------------|
| Quaternary ammonium salt | TEMAM : Triethylmethylammonium Hydrogen Maleate  TMAP : Tetramethylammonium Hydrogen Phthalate  |
| Tertiary ammonium salt | MA.TEA : Triethylammonium Hydrogen Maleate  |
| Simple ammonium salt | AA.A : Diammonium Adipate $\text{H}_4\text{N}^+ \text{ } ^-\text{OOC}(\text{CH}_2)_4\text{COO}^- \text{ } ^+\text{NH}_4$ |

The electrolytic conductivities of the new electrolytes are two or three times higher than those of the traditional electrolytes at practical concentrations as given in Table 4. Concentration dependence of electrolytic conductivities is shown in Fig. 6. The electrolytic conductivity generally increases with concentration, reaches its maximum and then decreases due to ionic association. The high electrolytic conductivities of the quaternary ammonium carboxylate/ γ -butyrolactone electrolytes are based on the high solubility and dissociating ability of the quaternary ammonium carboxylate salts. Temperature dependence of electrolytic conductivities is shown in Fig. 7. The new electrolytes do not freeze even at -55°C and show some conductivity, which is also based on the high solubility of the quaternary ammonium carboxylate salts.

Table 4. Comparison of electrolytic conductivities at 25°C .

| Electrolyte | C / wt% | σ / mS cm^{-1} |
|--------------|-----------|--------------------------------|
| TEMAM / GBL | 25 | 14.5 |
| TMAP / GBL | 25 | 10.1 |
| MA.TEA / GBL | 25 | 4.6 |
| AA.A / EG | 10 | 3.2 |

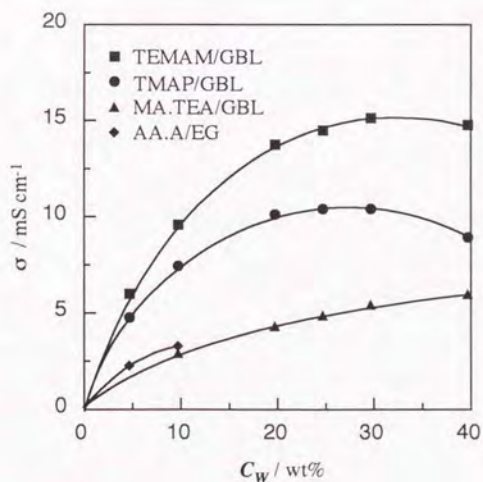


Fig. 6. Concentration dependence of electrolytic conductivities at 25°C .

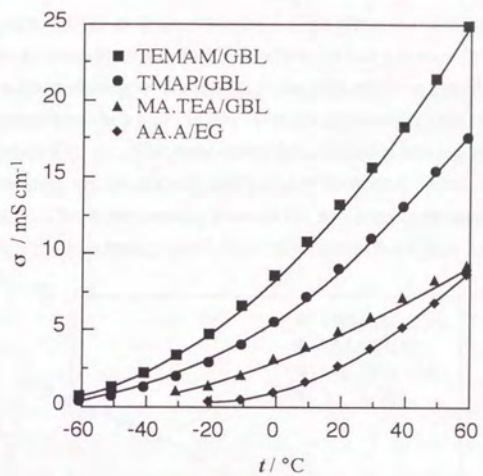


Fig. 7. Temperature dependence of electrolytic conductivities.

The another character of the new electrolytes is high chemical stability. Fig. 8 shows the deterioration of electrolytic conductivity at 25°C, when electrolytes were left at 115°C for a long period. Ammonium adipate undergoes the esterification with ethylene glycol solvent and results in the deposition of adipamide as shown in Fig. 9a. Tertiary ammonium salts tend to lose amines by evaporation as shown in Fig. 9b. The new electrolyte deteriorates slowly than the traditional electrolytes. Particularly, the quaternary ammonium hydrogen phthalate electrolyte shows amazingly high stability. This is presumably because the decomposition reaction shown in Fig. 9c, is suppressed by high activation energy for C-N bond scission (See Chap. 2.8.).

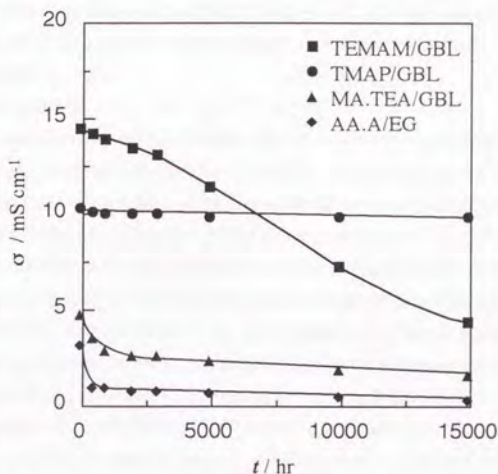


Fig. 8. Deterioration of electrolytic conductivities at 25°C caused by heat at 115°C.

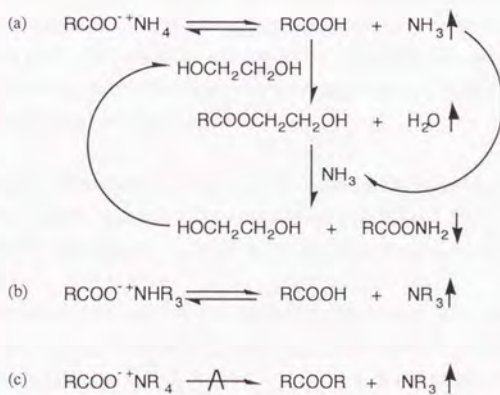


Fig. 9. Deterioration mechanisms of the electrolytes.

2.4. Conductometric Analysis of Quaternary Ammonium Salts

In the previous chapters, it was shown that quaternary ammonium salts of carboxylic acids in γ -butyrolactone have acquired a potential application in aluminum electrolytic capacitors.

However, the conductivity data for quaternary ammonium carboxylates have been reported only for acetonitrile (AN) [12 - 14], N,N-dimethylformamide (DMF) [15 - 17] and propylene carbonate (PC) [18].

Therefore, a systematic study on the transport properties of quaternary ammonium carboxylate/ γ -butyrolactone electrolytes was carried out. The conductivity data of several quaternary ammonium bimalates, biphthalates and benzoates, which involve symmetric and asymmetric cations from tetramethylammonium to tetraethylammonium, are presented.

2.4.1. Experimental

Electrolyte preparation

Tetraethylammonium bimalate, biphthalate and benzoate were prepared by the neutralization of maleic acid (Tokyo Chemical Industry Co.), phthalic acid (Tokyo Chemical Industry Co.) and benzoic acid (Wako Pure Chemical Industries) with 40 wt % tetraethylammonium hydroxide aqueous solution (SACEM Inc., Ultapure grade). Tetramethylammonium bimalate, biphthalate and benzoate were prepared by the neutralization of the acids with tetramethylammonium bicarbonate aqueous solution obtained from the reaction of trimethylamine with dimethyl carbonate in methanol. Asymmetric quaternary ammonium bimalates, biphthalates and benzoates were prepared similarly using asymmetric quaternary ammonium bicarbonate aqueous solutions obtained from the reaction of appropriate amines with dimethyl carbonate.

The exact concentrations of quaternary ammonium hydroxide and bicarbonate aqueous solutions were determined by potentiometric titration with a standard sulfuric acid aqueous solution using an auto titrator (Hiranuma Sangyo Co., COMTITE-8/UCB-7).

These salts were dissolved in γ -butyrolactone (Mitsubishi Petrochemical Co., F-GBL). The solutions were then vacuum dried until the water content dropped below 500 ppm, and were readjusted to desired concentrations by adding appropriate amount of the solvent. Impurities in these stock solutions were determined by a X-ray fluorescence spectrometer (Rigaku Industrial Corp., 3370E) for Cl and an atomic absorption spectrometer (Hitachi, Z-9000) for Na, K and Fe. These impurities were found less than 1 ppm.

Measurements

The water contents in these stock solutions were measured by a moisture meter (Mitsubishi Kasei Co., CA-06). Their conductivities and densities at $25 \pm 0.1^\circ\text{C}$ were measured by a conductivity meter (Toa Electronics, CM-30S/CGT-511B) and a digital density meter (PAAR, DMA 45), respectively.

The stock solutions were successively diluted and the molar concentrations C (mol dm^{-3}) were calculated from concentrations m' (mol kg^{-1} -solution) and densities d (g cm^{-3}) by $C = m'd$. The densities were calculated from $d = d_o + Dm'$, where d_o is the density of solvent and D is a characteristic constant of the electrolyte.

The conductivity measurements were carried out at $25 \pm 0.1^\circ\text{C}$ by a bridge (Toa Electronics,

CM-25E) and a standard type conductivity cell with a cell constant 0.104 cm^{-1} (Toa Electronics, CG-2001PL). The molar conductivities Λ were calculated from the experimental electrolytic conductivities after correction for the electrolytic conductivity of the solvent.

Density, viscosity, relative permittivity and electrolytic conductivity of γ -butyrolactone are 1.1248 g cm^{-3} , $1.727 \times 10^{-2} \text{ P}$ [19], 41.77 [19] and $2.5 \times 10^{-7} \text{ S cm}^{-1}$, respectively.

Molecular modeling

The ionic sizes were calculated from the molecular models constructed by a molecular modeling system CHEMLAB-II (Molecular Design Co.) on a VAX8350 (Digital Equipment Corp.). The MM2 program was used for structure optimization.

2.4.2. Results and Discussion

Molar conductivities

During the course of pursuing an electrolyte which exhibits the highest conductivity, the structural optimization of a cation in quaternary ammonium carboxylate/ γ -butyrolactone electrolytes has been carried out. Triethylmethylammonium salts have shown lower conductivities than tetraethylammonium counterparts at higher solute concentrations, particularly for benzoate electrolytes as shown in Fig. 10, where electrolytic conductivities σ of each electrolyte are plotted against solute concentration C_w . The conductivities and densities of the 1 mol dm^{-3} solutions of quaternary ammonium bimalates, biphthalates and benzoates are given in Table 5 and Table 6, respectively. The concentrations of tetramethylammonium bimalate, tetramethylammonium benzoate and trimethylethylammonium benzoate were adjusted to 0.1 mol dm^{-3} due to their low solubility in γ -butyrolactone. The molar conductivities over the concentration range of 10^{-2} to $10^{-3} \text{ mol dm}^{-3}$ are given in Table 7.

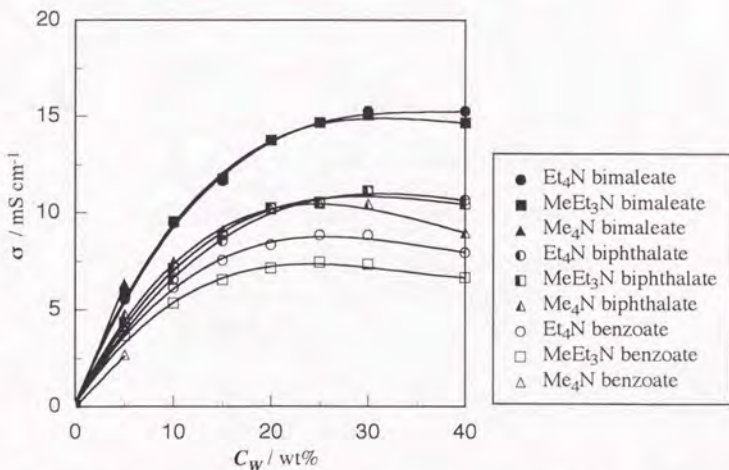
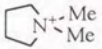


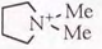
Fig. 10. Concentration dependence of the conductivities of quaternary ammonium carboxylate/GBL electrolytes at 25°C .

Table 5. Conductivities of 1 mol dm⁻³ quaternary ammonium carboxylate/GBL electrolytes at 25°C.

| σ / mS cm ⁻¹ |  |  |  |
|-----------------------------------------------------------------------------------|-----------------------------------------------------------------------------------|-----------------------------------------------------------------------------------|-----------------------------------------------------------------------------------|
| Me ₄ N ⁺ | 2.7* | 10.1 | 1.5* |
| Me ₃ EtN ⁺ | 12.9 | 10.5 | 1.6* |
|  | 13.3 | 10.5 | 5.9 |
| Me ₂ Et ₂ N ⁺ | 13.7 | 10.8 | 6.0 |
| MeEt ₃ N ⁺ | 13.7 | 10.8 | 6.8 |
| Et ₄ N ⁺ | 13.8 | 10.5 | 8.3 |

* 0.1 mol dm⁻³

Table 6. Densities of 1 mol dm⁻³ quaternary ammonium carboxylate/GBL electrolytes at 25°C.

| d / g cm ⁻³ |  |  |  |
|------------------------------------------------------------------------------------|-----------------------------------------------------------------------------------|-----------------------------------------------------------------------------------|-----------------------------------------------------------------------------------|
| Me ₄ N ⁺ | 1.1241* | 1.1404 | 1.1231* |
| Me ₃ EtN ⁺ | 1.1279 | 1.1379 | 1.1230* |
|  | 1.1362 | 1.1453 | 1.1260 |
| Me ₂ Et ₂ N ⁺ | 1.1249 | 1.1346 | 1.1157 |
| MeEt ₃ N ⁺ | 1.1227 | 1.1324 | 1.1149 |
| Et ₄ N ⁺ | 1.1200 | 1.1300 | 1.1128 |

* 0.1 mol dm⁻³

Table 7. Molar concentrations and molar conductivities of quaternary ammonium carboxylate/GBL electrolytes at 25°C.

| $10^3 C$ / mol dm ⁻³ | Λ / S cm ² mol ⁻¹ | $10^3 C$ | Λ | $10^3 C$ | Λ |
|------------------------------------------------------------------------------------------------|----------------------------------------------------|---------------------------------------------------------------------------------------------------|-----------|------------------------------------------------------------------------------------------------|-----------|
| Me ₄ N bimalate | | Me ₄ N biphthalate | | Me ₄ N benzoate | |
| 9.7352 | 40.189 | 9.9677 | 35.540 | 9.9975 | 29.482 |
| 7.7479 | 40.960 | 7.9319 | 36.618 | 8.3015 | 30.543 |
| 5.9551 | 41.922 | 6.1130 | 37.322 | 6.1986 | 32.193 |
| 3.6390 | 43.157 | 4.1578 | 38.349 | 4.3194 | 34.044 |
| 1.9542 | 44.469 | 2.1405 | 39.869 | 2.0599 | 36.415 |
| 1.0916 | 45.437 | 1.1319 | 40.656 | 1.0337 | 37.720 |
| Me ₃ EtN bimalate | | Me ₃ EtN biphthalate | | Me ₃ EtN benzoate | |
| 9.7407 | 39.756 | 10.0582 | 36.015 | 9.9984 | 30.460 |
| 8.2007 | 40.405 | 8.0444 | 36.752 | 7.9466 | 31.869 |
| 6.3841 | 41.236 | 6.0054 | 37.508 | 5.9711 | 33.286 |
| 4.3085 | 42.347 | 4.0345 | 38.775 | 4.1141 | 34.819 |
| 1.9471 | 43.928 | 2.0391 | 39.773 | 2.0683 | 36.808 |
| 0.9751 | 44.938 | 1.0332 | 40.749 | 1.0424 | 37.683 |
|  -Me bimalate | |  -Me biphthalate | |  -Me benzoate | |
| 9.9679 | 39.462 | 9.7567 | 35.939 | 10.0056 | 31.168 |
| 8.3737 | 40.060 | 7.9368 | 36.595 | 8.0117 | 32.321 |
| 6.5422 | 40.911 | 6.0204 | 37.348 | 5.9877 | 33.628 |
| 4.5274 | 41.934 | 4.0393 | 38.410 | 4.0557 | 35.148 |
| 2.5150 | 43.121 | 1.9767 | 39.606 | 1.9935 | 36.996 |
| 1.2196 | 44.300 | 1.0320 | 40.376 | 1.0259 | 37.616 |
| Me ₂ Et ₂ N bimalate | | Me ₂ Et ₂ N biphthalate | | Me ₂ Et ₂ N benzoate | |
| 9.9887 | 38.949 | 9.8348 | 35.583 | 10.0892 | 31.682 |
| 7.9113 | 39.874 | 7.9977 | 36.204 | 7.9887 | 32.715 |
| 5.8964 | 40.695 | 6.1726 | 36.994 | 6.0493 | 33.830 |
| 3.9468 | 41.768 | 4.2241 | 37.937 | 4.1092 | 35.177 |
| 1.9774 | 42.874 | 2.0479 | 39.187 | 2.0969 | 36.936 |
| 1.0196 | 43.921 | 1.0576 | 39.997 | 1.1204 | 37.676 |
| MeEt ₃ N bimalate | | MeEt ₃ N biphthalate | | MeEt ₃ N benzoate | |
| 9.9253 | 38.815 | 9.9849 | 35.113 | 9.9857 | 32.401 |
| 7.9012 | 39.481 | 8.3456 | 35.534 | 7.9811 | 33.323 |
| 6.0870 | 40.159 | 6.4731 | 36.157 | 6.1242 | 34.282 |
| 4.1749 | 41.091 | 4.4558 | 37.019 | 4.1484 | 35.447 |
| 2.0363 | 42.459 | 2.4753 | 38.146 | 2.0322 | 36.792 |
| 1.0099 | 43.391 | 1.2917 | 39.149 | 1.0127 | 37.455 |
| Et ₄ N bimalate | | Et ₄ N biphthalate | | Et ₄ N benzoate | |
| 9.8916 | 38.755 | 9.9316 | 34.491 | 10.1772 | 32.666 |
| 7.7222 | 39.477 | 8.1159 | 35.049 | 8.2609 | 33.344 |
| 5.8570 | 40.132 | 5.9566 | 35.885 | 6.3718 | 34.048 |
| 3.7297 | 41.116 | 4.0016 | 36.623 | 4.4023 | 34.902 |
| 2.0008 | 42.209 | 2.6788 | 37.218 | 2.4429 | 36.023 |
| 1.0265 | 43.011 | 1.4889 | 38.082 | 1.2805 | 36.792 |

Analysis of conductivity data

The conductivity data were analyzed by means of the Fernández-Prini expansion of the Fuoss-Hsia equation (See Chap. 6). Derived parameters are summarized in Table 8 and Table 9.

Table 8. Derived limiting molar conductivities.

| Λ_0 / S cm ² mol ⁻¹ |  |  |  |
|------------------------------------------------------------------------------------------------------------|-----------------------------------------------------------------------------------|-----------------------------------------------------------------------------------|-----------------------------------------------------------------------------------|
| Me ₄ N ⁺ | 48.15 | 43.47 | 41.55 |
| Me ₃ EtN ⁺ | 47.50 | 43.25 | 41.26 |
|  N ⁺ -Me Me | 47.13 | 42.87 | 40.94 |
| Me ₂ Et ₂ N ⁺ | 46.43 | 42.49 | 40.86 |
| MeEt ₃ N ⁺ | 45.82 | 41.69 | 40.20 |
| Et ₄ N ⁺ | 45.42 | 40.78 | 39.46 |

Table 9. Derived association constants.

| K_A / dm ³ mol ⁻¹ |  |  |  |
|--------------------------------------------------------------------------------------------------------------|-----------------------------------------------------------------------------------|-----------------------------------------------------------------------------------|-----------------------------------------------------------------------------------|
| Me ₄ N ⁺ | 12.87 | 14.27 | 47.65 |
| Me ₃ EtN ⁺ | 11.83 | 11.00 | 35.50 |
|  N ⁺ -Me Me | 11.37 | 10.00 | 28.39 |
| Me ₂ Et ₂ N ⁺ | 10.36 | 10.00 | 24.68 |
| MeEt ₃ N ⁺ | 9.06 | 9.03 | 15.64 |
| Et ₄ N ⁺ | 7.44 | 7.34 | 10.38 |

Single ion limiting molar conductivities

The consistent set of the single ion limiting molar conductivities of quaternary ammonium ions and carboxylate ions are given in Table 10, where $\lambda_o^-(\text{Et}_4\text{N}^+) = 19.32$ is used for calculation (See Chap. 4.3).

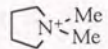
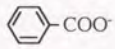
Walden products $\lambda_o\eta$ of each ion are plotted against the reciprocal of ionic radius r in Fig. 11. The theoretical behavior calculated from Stokes law is given by the bottom line for perfect stick and by the top line for perfect slip. All ions nearly follow the theoretical behavior for perfect slip, which suggests that they are able to move without adhesion to γ -butyrolactone. The inversion of the order in the mobility between biphthalate and benzoate ion, which cannot be seen in the aqueous solution [20], may be explained by the lower conductivity of benzoate solution over the experimental concentration range due to the ion association discussed later.

Association constants

Derived ion association constants in Table 9 are plotted against ionic radii of cations as shown in Fig. 12. The K_A values increase in the order, $\text{Et}_4\text{N}^+ < \text{MeEt}_3\text{N}^+ < \text{Me}_2\text{Et}_2\text{N}^+ < \text{Me}_2(\text{CH}_2)_4\text{N}^+ < \text{Me}_3\text{EtN}^+ < \text{Me}_4\text{N}^+$ with decreasing cation size. This tendency can be predicted theoretically by the Bjerrum equation. Calculated K_B values are shown by the broken curves in Fig. 12. The fact that the K_B values are smaller than the experimental K_A values indicates the existence of ion-dipole and dipole-dipole interaction besides an electrostatic force due to the delocalizability of the carboxylate ions.

A large dependence of cation size on the ion association constant observed for benzoate solutions cannot be explained theoretically. However this result is closely related to the low ionization constant Ka of benzoic acid in γ -butyrolactone compared with maleic acid and phthalic acid.

Table 10. Single ion limiting molar conductivities.

| λ_o^+ / S cm ² mol ⁻¹ | | λ_o^- / S cm ² mol ⁻¹ | |
|-------------------------------------------------------------------------------------|------|-------------------------------------------------------------------------------------|------|
| Me_4N^+ | 21.8 |  | 26.1 |
| Me_3EtN^+ | 21.5 |  | 21.5 |
|  | 21.1 |  | 20.1 |
| $\text{Me}_2\text{Et}_2\text{N}^+$ | 20.7 | | |
| MeEt_3N^+ | 20.0 | | |
| Et_4N^+ | 19.3 | | |

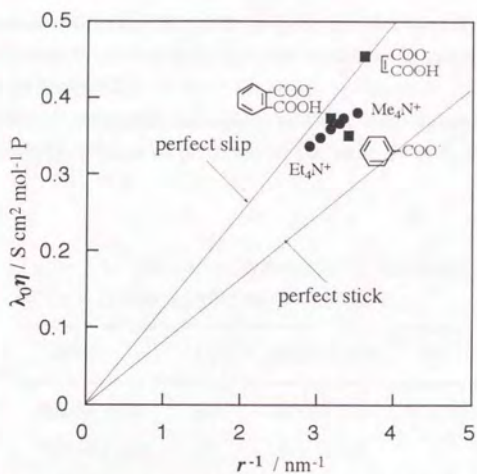


Fig. 11. Walden product as a function of the reciprocal of ionic radius.

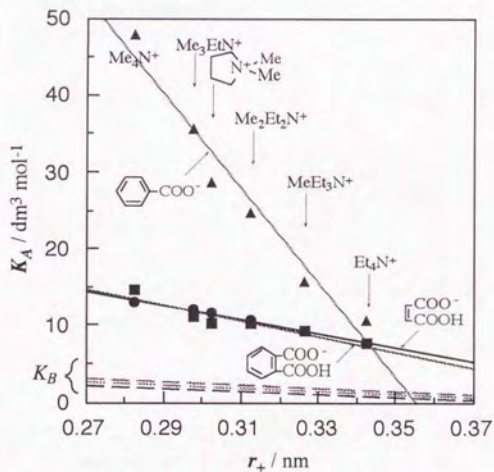


Fig. 12. Effect of cation size on association constants.

The ionization constants of carboxylic acids are given in Table 11 [21], where the values in γ -butyrolactone are estimated by the data that pK_a values in γ -butyrolactone are smaller than those in propylene carbonate by 2 units [22].

Lower conductivities of triethylammonium salts than tetraethylammonium counterparts at higher concentrations (Fig. 10) can be predicted by the tendency of K_A values obtained at low concentrations.

Table 11. Ionization constants of carboxylic acids in dipolar aprotic solvents at 25°C.

| pK_{a1} | GBL* ¹ | DMA* ² | AN | PC |
|----------------|-------------------|-------------------|----|----|
| Maleic acid | 10 | 4 | - | - |
| Phthalic acid | 11 | 5 | 14 | - |
| Salicylic acid | 14 | 7 | 17 | 15 |
| Benzoic acid | 18 | 11 | 21 | 20 |

*¹ Estimated values

*² Dimethylacetamide

2.5. Conductometric Analysis of Tertiary Ammonium Salts

The conductometric study was extended to the tertiary ammonium carboxylates in order to clarify the difference in ionic association between tertiary and quaternary ammonium salts.

The conductometric analysis of tertiary ammonium salts in γ -butyrolactone has not been reported and only the data for diethylammonium salicylate [23, 24] (secondary ammonium salt) have been published.

2.5.1. Experimental

Triethylammonium bimaleate, biphthalate and benzoate were prepared *in situ* by the neutralization of maleic acid, phthalic acid and benzoic acid with triethylamine in γ -butyrolactone.

Triethylammonium perchlorate and triethylammonium tetrafluoroborate were prepared by the titration of aqueous perchloric acid and tetrafluoroboric acid with triethylamine, respectively, followed by recrystallization and vacuum drying.

The water content in the mother solutions (less than 100 ppm) was measured by a moisture meter and the concentrations of the solutions were calibrated. The conductivity measurements were carried out by the method described before.

2.5.2. Results and Discussion

Molar conductivities

The molar conductivities Λ of 1 mol dm^{-3} tertiary ammonium salts are given in Table 12 and those of the corresponding quaternary ammonium counterparts are also given for reference. The molar conductivities of the triethylammonium carboxylates were evidently lower than those of the corresponding diethyldimethylammonium carboxylates having the same formula weight, on the other hand, this was not true when the counter anion was replaced with a strong electron withdrawing anion.

The molar conductivities of the diluted solutions (C ; 10^{-2} to $10^{-3} \text{ mol dm}^{-3}$) are given in Table 13. The difference in molar conductivity between triethylammonium and diethyldimethylammonium carboxylates increased with increasing concentration due to ionic association as shown in Fig. 13.

Analysis of conductivity data

The conductivity data were analyzed by means of the Fernández-Prini expansion of the Fuoss-Hsia equation (See Chap. 6). Derived parameters are summarized in Table 14 and Table 15.

Table 12. Comparison of molar conductivities of 1 mol dm^{-3} tertiary and quaternary ammonium salts in GBL at 25°C .

| Λ / $S \text{ cm}^2 \text{ mol}^{-1}$ |  COO^- COOH |  COO^- COOH |  COO^- | ClO_4^- | BF_4^- |
|--------------------------------------------------|---------------------------------------------------------------------------------------------------------------------|---------------------------------------------------------------------------------------------------------------------|----------------------------------------------------------------------------------------------------|------------------|-----------------|
| Et_3NH^+ | 4.1 | 3.2 | 0.4 | 16.7 | 18.2 |
| $\text{Me}_2\text{Et}_2\text{N}^+$ | 13.7 | 10.8 | 6.0 | | |
| Et_4N^+ | 13.8 | 10.5 | 8.3 | 15.9 | 17.8 |

Table 13. Molar concentrations and molar conductivities of tertiary ammonium salts in GBL at 25°C.

| $10^3 C$ / mol dm ⁻³ | Λ / S cm ² mol ⁻¹ | $10^3 C$ | Λ |
|------------------------------------|----------------------------------------------------|-----------------------------------|-----------|
| Et ₃ NHbimalate | | Et ₃ NHbipthalate | |
| 7.9653 | 22.943 | 8.1833 | 20.536 |
| 5.9730 | 24.853 | 6.1357 | 22.353 |
| 3.9813 | 27.591 | 4.0923 | 24.839 |
| 1.9932 | 32.210 | 2.0497 | 28.932 |
| 1.3965 | 34.049 | 1.4343 | 30.748 |
| 0.7999 | 36.815 | 0.8210 | 33.374 |
| Et ₃ NHbenzoate | | | |
| 8.1956 | 2.010 | | |
| 6.1461 | 2.127 | | |
| 4.0987 | 2.281 | | |
| 2.0493 | 2.513 | | |
| 1.4367 | 2.655 | | |
| 0.8205 | 2.858 | | |
| Et ₃ NHClO ₄ | | Et ₃ NHBF ₄ | |
| 10.0060 | 41.230 | 10.3405 | 43.001 |
| 7.5052 | 42.111 | 7.7544 | 43.969 |
| 5.0067 | 43.272 | 5.1706 | 45.227 |
| 2.5054 | 44.963 | 2.5866 | 47.031 |
| 1.7555 | 45.629 | 1.8145 | 47.726 |
| 1.0031 | 46.307 | 1.0420 | 48.512 |

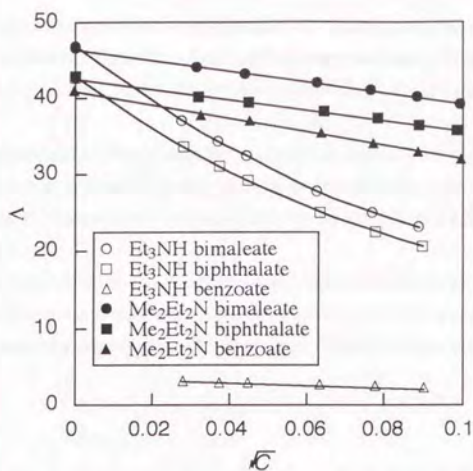


Fig. 13. Kohlrausch plots for tertiary and quaternary ammonium carboxylates in GBL at 25°C.

Table 14. Derived limiting molar conductivities.

| Λ_0 / S cm ² mol ⁻¹ | <chem>[O-]C(=O)C(=O)O</chem> | <chem>O=C(O)c1ccccc1</chem> | <chem>O=C(O)c1ccc(cc1)C(=O)[O-]</chem> | <chem>[O-]C(=O)C(=O)[O-]</chem> | <chem>[O-]F(B)(F)F</chem> |
|------------------------------------------------------|------------------------------|-----------------------------|----------------------------------------|---------------------------------|---------------------------|
| Et ₃ NH ⁺ | 43.62 (46.54) | 39.72 (41.90) | - | 48.94 | 51.28 |
| Me ₂ Et ₂ N ⁺ | 46.43 | 42.49 | 40.86 | | |
| Et ₄ N ⁺ | 45.42 | 40.78 | 39.46 | 47.77 | 50.19 |

Table 15. Derived association constants.

| K_A / dm ³ mol ⁻¹ | <chem>[O-]C(=O)C(=O)O</chem> | <chem>O=C(O)c1ccccc1</chem> | <chem>O=C(O)c1ccc(cc1)C(=O)[O-]</chem> | <chem>[O-]C(=O)C(=O)[O-]</chem> | <chem>[O-]F(B)(F)F</chem> |
|------------------------------------------------|------------------------------|-----------------------------|----------------------------------------|---------------------------------|---------------------------|
| Et ₃ NH ⁺ | 226.2 | 228.0 | - | 11.0 | 11.9 |
| Me ₂ Et ₂ N ⁺ | 10.4 | 10.0 | 24.7 | | |
| Et ₄ N ⁺ | 7.4 | 7.3 | 10.4 | 9.5 | 9.9 |

Lower limiting molar conductivities were obtained for tertiary ammonium carboxylates due to the large association constants. Therefore, their limiting molar conductivities were estimated from the data of $\text{Et}_3\text{NHClO}_4$, which showed a slight association. These values are given in parentheses in Table 14.

The association constants of the triethylammonium carboxylates were more than 20 times higher than those of the corresponding diethylmethylammonium salts having the same formula weights. Extraordinarily large ionic association prohibited the simple calculation for the triethylammonium benzoate.

This behavior can be ascribed to the hydrogen bond effect of a protic cation. It is evident that there is a large difference in ionic association between protic cation (tertiary ammonium ion) and non-protic cation (quaternary ammonium ion) in the case of carboxylate salts.

2.6. Anodic Oxidation of Aluminum in Organic Electrolytes

A great number of studies on anodization of aluminum in aqueous electrolytes have been reported, however, investigations in nonaqueous electrolytes are very limited [25 - 27]. A nonaqueous electrolyte is used inside an aluminum electrolytic capacitor as a true cathode, which is directly in contact with a pre-anodized aluminum foil. Because the nonaqueous electrolyte plays a decisive role in repairing the defects of the oxide film in the capacitor, detailed knowledge of its film forming ability is required to get a highly reliable capacitor [28].

Nonaqueous solvents including formamide [29, 30], N-methylformamide [31], N,N-dimethylformamide [32 - 35], dimethylsulfoxide [36, 37], ethylene glycol [33 - 35, 38 - 40], ethylene carbonate-based mixed solvents [41], ethanol [42], dioxane [43, 44] and pyridine [45] were used for anodization of aluminum, however, most electrolytes included a considerable amount of water. Little attention has been paid to the amount of contaminated water in the electrolyte [46].

The present study concerns the film forming ability of the highly conductive electrolytes consisting of a quaternary ammonium carboxylate and γ -butyrolactone, which we have developed for low-impedance capacitors. The film breakdown voltage, film forming coulomb efficiency, and film forming speed were examined with respect to the kind of carboxylate anion, its concentration and the water concentration in the electrolyte.

2.6.1. Experimental

Three kinds of quaternary ammonium carboxylate/ γ -butyrolactone electrolytes (Mitsubishi Petrochemical Co.) were used. The following abbreviations were used for solutes and solvent: triethylmethylammonium hydrogen maleate (TEMAM), tetramethylammonium hydrogen phthalate (TMAP), triethylmethylammonium benzoate (TEMAB) and γ -butyrolactone (GBL). These electrolytes were vacuum dried when required and the water content and conductivity were measured by a moisture meter (Mitsubishi Kasei Co., CA-06) and a conductivity meter (Toa Electronics, CM-30S), respectively.

A smooth aluminum foil of 100 μm thickness and 99.99 % purity (Mitsubishi Aluminum Co.) was cut into a 10 x 20 mm rectangle with a thin long tag for electrical contact. This flag shape coupon was degreased in acetone, chemically polished in 0.1 mol dm^{-3} - NaOH aqueous solution for 10 min at room temperature, and washed with pure water, followed by rinsing with acetone and by drying in air.

The anodization of the coupon was usually carried out in an aluminum tube cell, having dimensions of 15 mm in inner diameter and 35 mm in height, and containing 5 g of the electrolyte. When the effect of the water content in the electrolyte was examined, the anodization was performed in an argon glove box (Eicho Shokai Co., VDB-CB-6311Y) equipped with a moisture removing apparatus (Vacuum Atmosphere Co., HE-493) and a glass beaker cell with a stainless steel foil cathode containing 20 g of the electrolyte was used to avoid contaminating the aluminum from the cathode. The amount of dissolved aluminum ion in the electrolyte was determined by an atomic absorption spectrometer (Hitachi, Z-9000).

A constant current power source (Kikusui Electronics Co., PAD500-2L) was used for the

galvanostatic anodization experiment, and the voltage across the cell was recorded on an intelligent recorder (Toa Electronics, INR-6061). The differential of the cell voltage was also recorded by placing a differentiating circuit consisting of a $0.1 \mu\text{F}$ capacitor and a series $1 \text{ k}\Omega$ resistor (time constant $100 \mu\text{s}$) in parallel with the cell. A function synthesizer (Toa Electronics, FS-2201) and a power amplifier (NF Circuit Design Block Co., 4310) were used for the voltastatic anodization experiment.

The morphology of the anodic oxide films was observed with a scanning electron microscope (Hitachi, S-900).

2.6.2. Results and Discussion

Formation of anodic oxide films

The galvanostatic formation of the anodic aluminum oxide film in the quaternary ammonium carboxylate/ γ -butyrolactone electrolytes proceeded by an increase in the formation voltage V_f with time t to the breakdown voltage V_b followed by an oscillation as shown in Fig. 14. The shape of the V_f - t curve, having generally a non-linear voltage increase, varied with a number of parameters, e.g. the composition and concentration of the electrolyte, its water content, current density, and temperature. The phthalate solution caused an unknown oscillation around 60 V under specific conditions.

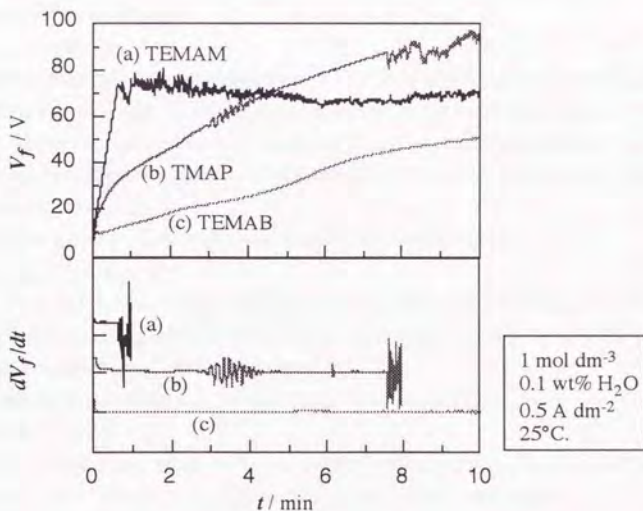


Fig. 14. Time dependence of the formation voltage during galvanostatic anodization of aluminum.

(a) Film breakdown voltage

It is well known that the breakdown voltage depends on the composition and concentration of the electrolyte and is expressed by the empirical equation 1:

$$V_b = a + b \log \rho \quad (1)$$

, where a and b are constants for a given electrolyte composition and ρ is the resistivity of the electrolyte [33].

The breakdown voltage was examined as a function of current density, temperature, electrolyte concentration and water concentration for the three electrolytes; maleate (TEMAM/GBL), phthalate (TMAP/GBL) and benzoate (TEMAB/GBL) solutions. The breakdown voltage proved to be slightly dependent on current density J and temperature T (Fig. 15), for example, their dependence for 1 mol dm⁻³-TMAP/GBL was given as follows:

$$\Delta V_f / \Delta(\log J) = -3 \quad (J = 0.01 - 10 \text{ A dm}^{-2})$$

$$\Delta V_f / \Delta(T/10) = -2 \quad (T = 25 - 125 \text{ }^\circ\text{C})$$

The effect of the electrolyte concentration was larger than the kind of carboxylate anion as shown in Fig. 16. The linear relationship of equation 1 was also confirmed in Fig. 17.

We have found the concentration of water in nonaqueous electrolyte became the third parameter to affect the breakdown voltage as shown in Fig. 18. The maleate solution showed a tendency to give a little bit higher breakdown voltage at lower water content, on the other hand, the phthalate solution showed higher value at higher water content. Although the benzoate solution could not attain the breakdown voltage at the high concentration of 1 mol dm⁻³, the maximum attained voltage increased with the water content.

(b) Film forming coulomb efficiency

Effect of parameters on the total charge passed from 0 V to 75 V of the formation voltage for TMAP/GBL solution is shown in Fig. 19. Since the increase rate of the formation voltage dV_f/dt largely depended on the kind of carboxylate anion as shown in Fig. 14, total charge passed from 0 V to 75 V of the formation voltage was plotted as a function of the electrolyte concentration (Fig. 20) and the water concentration (Fig. 21).

Total charge Q_t can be divided into several terms expressed in equation 2 [47]:

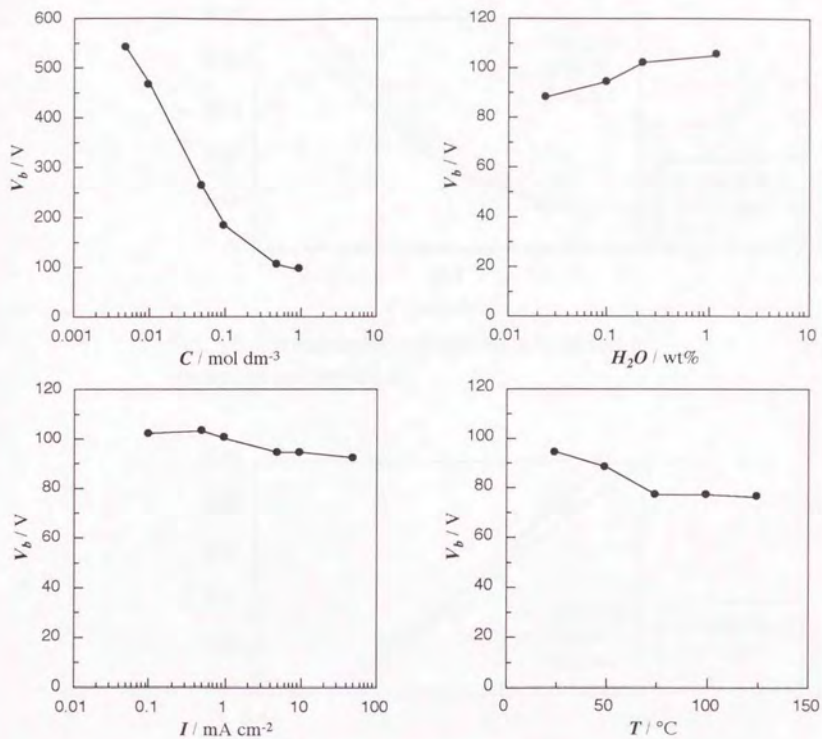
$$Q_t = Q_f + Q_d + Q_o + Q_r + Q_e \quad (2)$$

, where Q_f , Q_d , Q_o , Q_r and Q_e are the charge consumed by aluminum oxide formation, aluminum dissolution, oxygen generation due to water electrolysis, reaction of electrolyte solution and electronic conduction through the oxide film, respectively.

The charge used for the film formation Q_f is represented by equation 3 [47]:

$$Q_f = (nF/M)(V_f/E)dk \quad (3)$$

, where F is Faraday constant, n and M are valence and atomic weight of Al, and E , d , and k are electric field, density and Al³⁺ weight fraction of the aluminum oxide formed, respectively. The substitution of the typical values [47]; $d = 3 \text{ g cm}^{-3}$, $E = 0.77 \times 10^7 \text{ V cm}^{-1}$, and $k = 2 \text{ Al/Al}_2\text{O}_3 = 0.53$ gives $Q_f = 0.17 \text{ C cm}^{-2}$. Q_t for the maleate solution was 0.1 to 0.2 C cm⁻² as shown in Fig. 20 and 21, which indicates a good film forming coulomb efficiency. On the other hand, the phthalate and benzoate solution showed inferior efficiency particularly at low water concentration and high



Standard condition:

TMAP/GBL

$C = 1 \text{ mol dm}^{-3}$,

$H_2O = 0.1 \text{ wt\%}$,

$I = 0.5 \text{ A dm}^{-2}$,

$T = 25^\circ\text{C}$.

Fig. 15. Effect of parameters on breakdown voltage.

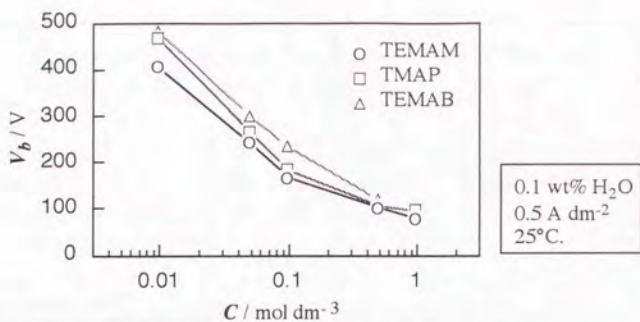


Fig. 16. Breakdown voltage as a function of electrolyte concentration.

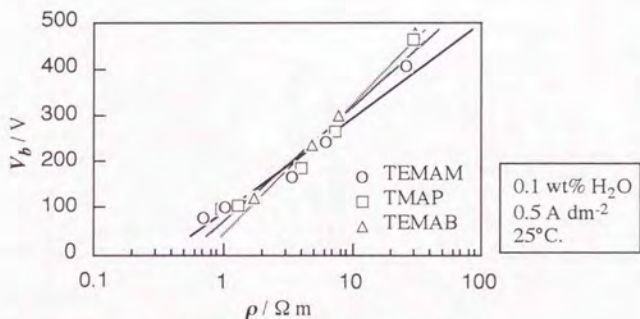


Fig. 17. Relationship between breakdown voltage and electrolyte resistivity.

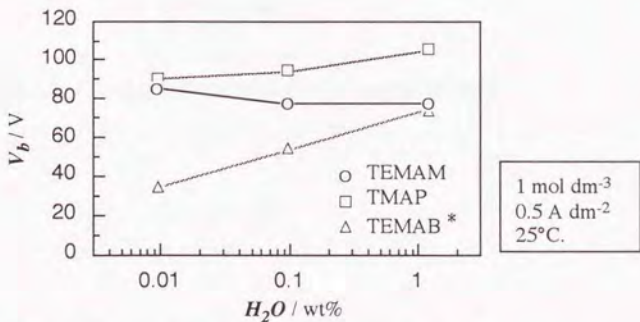
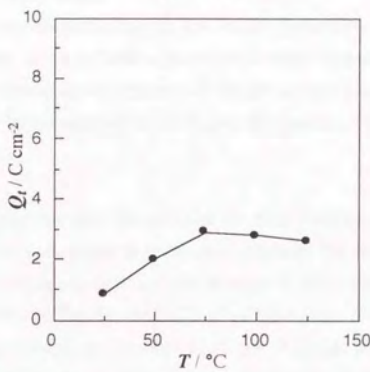
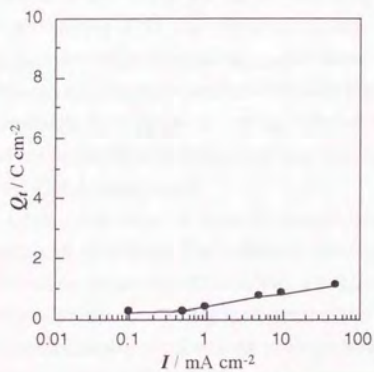
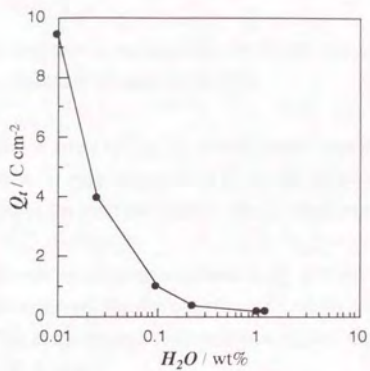
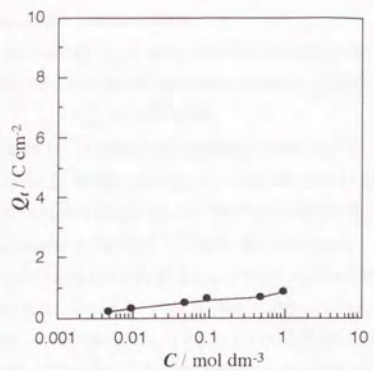


Fig. 18. Breakdown voltage as a function of water content. * Maximum voltage attained.



Standard condition:
 TMAP/GBL
 $C = 1 \text{ mol dm}^{-3}$,
 $H_2O = 0.1 \text{ wt}\%$,
 $I = 0.5 \text{ A dm}^{-2}$,
 $T = 25^\circ\text{C}$.

Fig. 19. Effect of parameters on total charge passed.

electrolyte concentration.

Excluding Q_p to elucidate the charge used, the dissolution of aluminum into the electrolyte was examined by atomic absorption analysis and Q_d was calculated by equation 4 [47]:

$$Q_d = (nF/M)W_d \quad (4)$$

, where W_d is weight of dissolved aluminum. The result is given in Fig. 22, whose feature was the same as Q_i shown in Fig. 21. The amount of Q_d accounts for only about 3 % of Q_i for the phthalate and benzoate solution and the dissolution of aluminum in the maleate solution was always below the detection limit of 0.1 ppm ($0.5 \mu\text{g cm}^{-2}$).

Although the oxygen gas evolution from the anode was seen during anodization, Q_o seemed to be small. Supposing all water in the electrolyte is electrolyzed, the consumption of 0.01 wt% of water by electrolysis is equivalent to 5.36 C cm^{-2} . This is not enough to compensate 9.39 C cm^{-2} obtained for the phthalate solution containing 0.01 wt% of water.

The coloring of the electrolyte and the film was observed particularly at low water concentration and high electrolyte concentration and this brown color darkened with a decrease in water content. Although no quantitative analysis has been made, Q_e caused by the reaction of the electrolyte must compensate for a larger part of Q_i , because Q_d can be considered to be negligibly small. The analysis of the decomposition products is in progress.

(c) Film forming speed

A non-linear increase in the formation voltage indicates that the speed of the film formation depends on the voltage. The voltastatic anodization was undertaken in order to supplement the data obtained by the galvanostatic mode. The current J_i during anodization was monitored at various potential sweep rates for the three electrolytes as shown in Fig. 23. At 0.5 V s^{-1} of sweep rate, the maleate solution showed no peak until the breakdown voltage, on the other hand, the phthalate and benzoate solution exhibited a rapid current increase before 50 V. Although the attribution of the peak leakage current is difficult, characterization of the film formed at each voltage is in progress.

The sweep rate which can give the current below 0.5 A dm^{-2} up to 75 V was conveniently adopted as the film forming speed. The film forming speed for each electrolyte was estimated as follows:

- TEMAM/GBL: 1.5 V s^{-1}
- > TMAP/GBL: 0.15 V s^{-1}
- > TEMAB/GBL: 0.05 V s^{-1} .

These values were very close to the calculated values of the slope between 0 V and 75 V on the $V_f - t$ curves in Fig. 14.

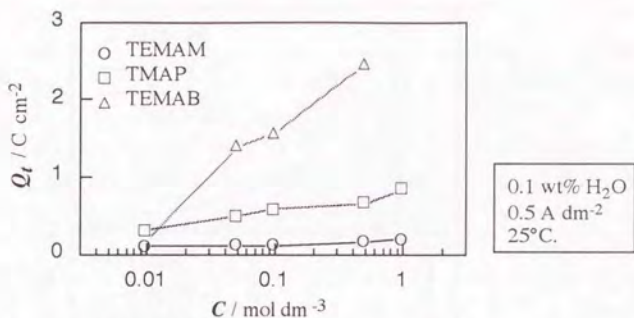


Fig. 20. Total charge passed as a function of electrolyte concentration.

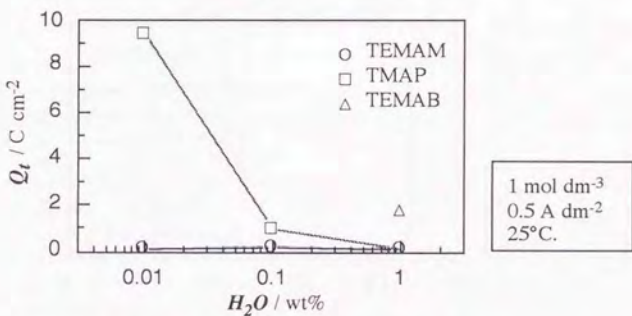


Fig. 21. Total charge passed as a function of water concentration.

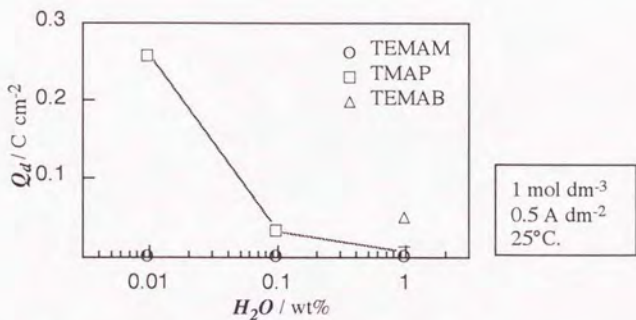


Fig. 22. Charge consumed for the dissolution of aluminum during anodization to 75 V.

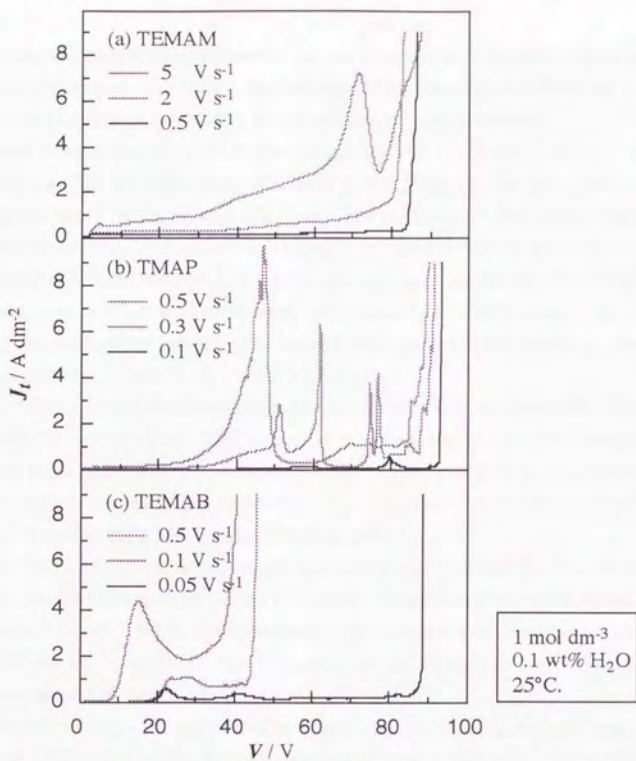


Fig. 21. Anodic polarization of aluminum at various potential sweep rates.

Film morphology

Morphology of the anodic oxide films obtained in the galvanostatic experiment was examined by a scanning electron microscope. The specimens were bent to see the cross section of the oxide film, and were observed without a metal coating at an accelerating voltage of 5 kV.

The maleate solution produced dense barrier-type films at both 0.01 wt% and 1 wt% of water content (Fig. 24a and 24b). The film obtained at 0.01 wt% of water attached firmly to aluminum base and the cross section could hardly be seen (Fig. 24a). The phthalate solution gave a porous-type film at 0.01 wt% of water (Fig. 24c) and a rough barrier-type film at 1 wt% of water (Fig. 24d). The benzoate solution, which could not attain 75 V at 0.1 wt% of water, produced another type of porous film (Fig. 24e). A barrier film with small pores was obtained at 1 wt% of water (Fig. 24f).

The smoothness of the anodic films formed in the three electrolytes was in the following order at the same water concentrations; TEMAM \gg TMAP $>$ TEMAB.

To make the water effect clearer, the forming voltage was raised to 90 V in 1 mol dm⁻³ - TMAP solution, at which scintillation began, and SEM images of the anodic oxide films were observed (Fig. 25). The smooth oxide film formed in an aqueous TMAP solution (Fig. 25a) was presented for reference. The formation of pores became marked as water concentration decreased (Fig. 25b and 25c), and eventually resulted in a fibrous structure (Fig. 25d).

The morphological changes with increasing voltage were shown in Fig. 26 for the films made in 1 mol dm⁻³ - TEMAM and TMAP solutions (water: 0.01 wt%). In the maleate solution, a barrier-type film was formed efficiently. While the aluminum oxide was successively built up in the phthalate solution resulting a fibrous porous-type film, accompanied by the decomposition of the solution (transport number of Al³⁺ can be close to 1).

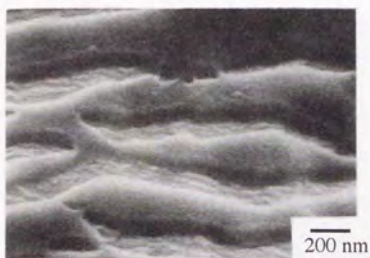
The buildup of a porous layer was closely related to Q_f , given in Table 16, where Q_f was roughly estimated by the equation 3. The low film forming coulomb efficiency observed in the phthalate solution has resulted mostly from the decomposition of the electrolyte and not from the generation of a porous-type layer, which consumed extra charge but did not serve to retain the voltage.

Table 16. Assignment of consumed charge .

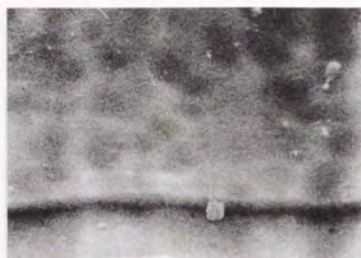
| V_f | TEMAM/GBL | | TMAP/GBL | | | |
|-------|-----------|--|----------|-------|-------|-----------------------|
| | Q_i | | Q_i | Q_f | Q_d | $Q_{o^+} Q_{r^+} Q_e$ |
| 25 | 0.03 | | 0.96 | 0.06 | 0.04 | 0.86 |
| 50 | 0.09 | | 4.28 | 0.11 | 0.18 | 3.99 |
| 75 | 0.12 | | 9.39 | 0.17 | 0.26 | 8.96 |
| 90 | 0.18 | | 15.77 | 0.20 | 0.41 | 15.16 |

in C cm⁻²

(a) 1 mol dm^{-3} TEMAM (0.01 wt% of water)



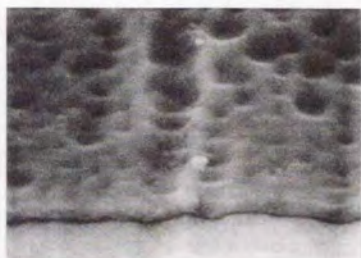
(b) 1 mol dm^{-3} TEMAM (1 wt% of water)



(c) 1 mol dm^{-3} TMAP (0.01 wt% of water)



(d) 1 mol dm^{-3} TMAP (1 wt% of water)



(e) 1 mol dm^{-3} TEMAB (0.1 wt% of water)



(f) 1 mol dm^{-3} TEMAB (1 wt% of water)



Fig. 24. SEM micrographs of the anodic films, $V_f = 75 \text{ V}$ (e; 54 V), $I = 0.5 \text{ A dm}^{-2}$.

(a) water solution (1 mol dm^{-3} TMAP)



(b) 1 wt% of water



(c) 0.1 wt% of water



(d) 0.01 wt% of water

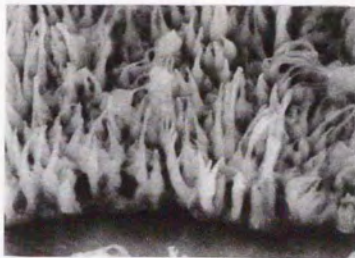


Fig. 25. Effect of water on film morphology,
 $V_f = 90 \text{ V}$, $I = 0.5 \text{ A dm}^{-2}$.

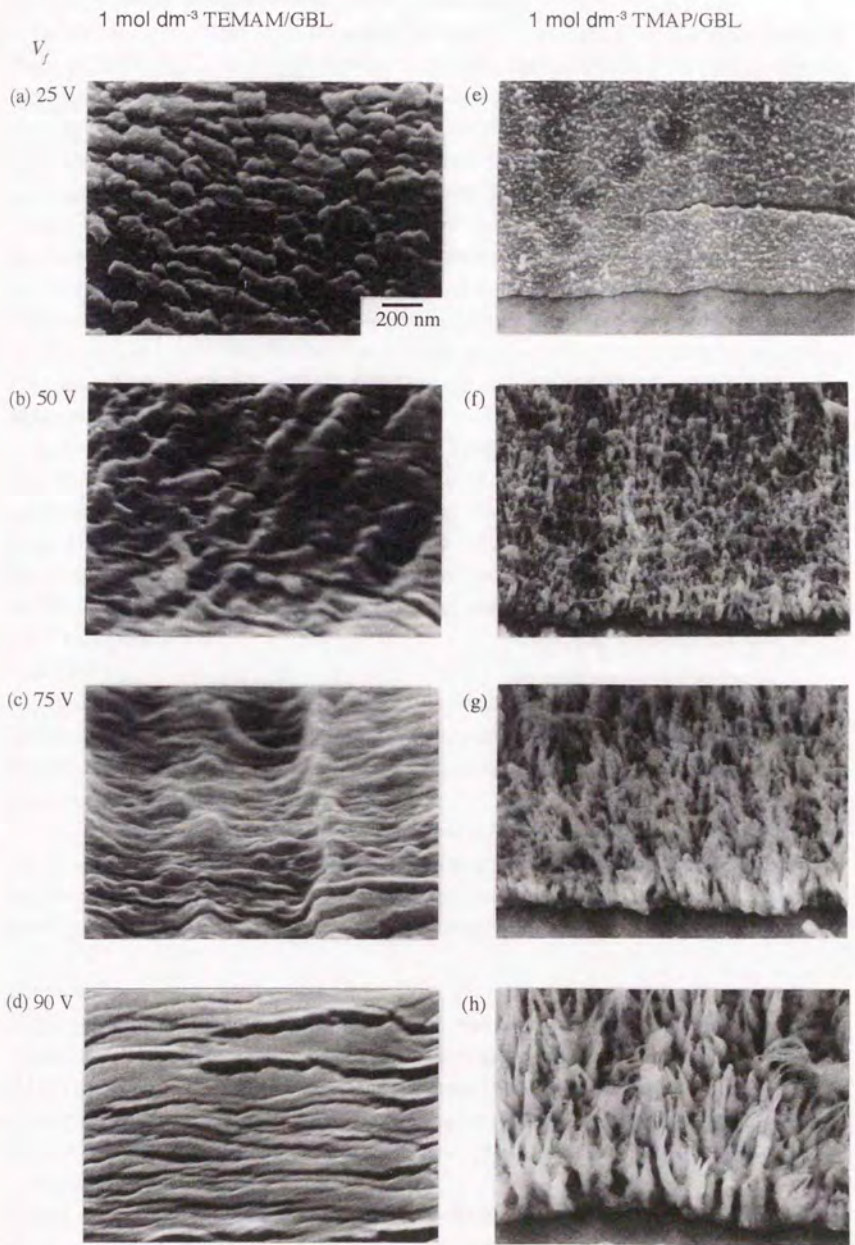


Fig. 26. Effect of formation voltage on film morphology, $I = 0.5 \text{ A dm}^{-2}$, 0.01 wt% of water.

2.7. Characterization of Aluminum Anodic Oxide Films

Incorporation of anions from the electrolyte solutions into the electrochemically grown aluminum oxide films is a well-known phenomenon [48]. The distribution of the various anions in the barrier films has been investigated by several groups to evaluate the properties of the films and to clarify the mechanism of film growth [49 - 63]. The incorporation of various anions including borate [40, 52 - 54, 57], phosphate [49 - 51, 55, 59, 61], tungstate [56, 58, 60], molybdate [60], manganate [60] and chromate [51, 60] has been studied. The general structure of the films has been reported to consist of a relatively pure inner region and an anion-containing outer region. The anion incorporation has also been reported in nonaqueous solutions such as ammonium pentaborate/ ethylenglycol [62, 63], boric acid/formamide [29] and ammonium tartrate/ethanol [42].

Recently the research on the anodic oxidation of aluminum has been extended to protophobic solvents such as γ -butyrolactone because quaternary ammonium carboxylate/ γ -butyrolactone electrolytes have acquired a potential application in high performance aluminum electrolytic capacitors.

In the previous section, it was shown that a small amount of water in the nonaqueous electrolytes has largely affected the coulomb efficiency for the anodic oxide film formation of aluminum and the morphology of the resultant film. This dependence was largely influenced by the kind of the carboxylate anion in the electrolyte. Maleate solution gave a barrier-type oxide film, while phthalate solution afforded a porous-type oxide layer under nearly anhydrous conditions. The present study is about a detailed characterization of these anodic oxide films.

2.7.1. Experimental

Materials

Two kinds of electrolyte solutions; 1 mol dm⁻³ triethylmethylammonium hydrogen maleate/ γ -butyrolactone (TEMAM/GBL) and tetramethylammonium hydrogen phthalate/ γ -butyrolactone (TMAP/GBL) (Mitsubishi Petrochemical Co., SOL-RITE KEM and KNP) were vacuum dried until water content dropped to 100 ppm.

A smooth aluminum foil of 100 μ m thickness and 99.99 % purity (Mitsubishi Aluminum Co.) was cut into a 20 x 50 mm rectangle with a thin long tag for electrical contact. These flag shape coupons were degreased in acetone, polished chemically in 0.1 mol dm⁻³ sodium hydroxide aqueous solution for 10 min at room temperature, washed with pure water, rinsed with acetone and dried.

Anodization

The galvanostatic anodization of the coupon was carried out in an aluminum tube cell containing an electrolyte solution placed in an argon glove box (Eicho Shokai Co., VDB-CB-6311Y) equipped with a moisture removing apparatus (Vacuum Atmospheres Co., HE-493). A constant current power source (Kikusui Electronics Co., PAD500-2L) was used and the voltage across the cell was recorded on an intelligent recorder (Toa Electronics, INR-6061).

Characterization

Fourier transform infrared spectroscopy (FT-IR; Nicolet, DX510), transmission electron microscopy (TEM; Hitachi H-7100FA), scanning transmission microscopy with allied energy

dispersive analysis of X-rays facilities (STEM/EDX; VG, HB501/KeveX, Delta plus) and Auger electron spectroscopy (AES; Ulvac-Phi, SAM-650) were used to observe the morphological and compositional characteristics of the films. The anodic films were isolated in 10% iodine-methanol solution and analyzed by a CHN elemental analyzer (Perkin-Elmer, 240C). The isolated films were dissolved in sulfuric acid and were analyzed by reverse phase liquid chromatography (Shimadzu, LC-9A).

2.7.2. Results and Discussion

The aluminum oxide films were formed at 0.5 A dm^{-2} up to 75 V in TEMAM/GBL and TMAP/GBL electrolytes containing either 0.01 wt% or 1 wt% of water.

(a) FT-IR

The FT-IR reflection spectra of the films in Fig. 27 indicated the existence of carboxylate anions, because a few peaks due to C=O stretching vibrations were observed in the region of $1740 - 1440 \text{ cm}^{-1}$ other than Al-O stretching around 920 cm^{-1} . The film, which was formed in TEMAM/GBL containing 0.01 wt% of water, had no remarkable peak due to Al-O stretching.

(b) TEM

The magnified images of the ultramicrotomed section of the films by TEM are given in Fig. 28. The thickness of barrier films formed in TEMAM/GBL and TMAP/GBL containing 1 wt% of water were about 80 nm and 90 nm, respectively (Fig. 28a and 28c). The anodization ratios of these films are calculated to be 1.1 and 1.2 nm V^{-1} , which are somewhat smaller than the values observed in aqueous solutions [47]. A barrier film formed in TEMAM/GBL containing 0.01 wt% of water was not uniform and its thickness ranged from 50 to 100 nm (Fig. 28b). A porous film formed in TMAP/GBL containing 0.01 wt% of water was 200 - 350 nm thick (Fig. 28d).

(c) STEM/EDX

Compositional feature of the ultramicrotomed section of the anodic oxide films was examined by STEM/EDX. X-ray data obtained from the probe positions shown in Fig. 29 are given in Table 17. Two series of measurements were carried out to show the reproducibility of the results [55].

The barrier films formed in TEMAM/GBL and TMAP/GBL containing 1 wt% of water (Fig. 29a and 29c) were hydrated aluminum oxides and the O/Al atomic ratio ranged from 1.6 to 4.3 (3 for $\text{Al}(\text{OH})_3$). The film formed in TEMAM/GBL containing 0.01 wt% of water (Fig. 29b) was found to be a composite aluminum oxide containing substantial amounts of maleate (O/Al = 1.2 - 1.9, C/Al = 2.4 - 7.4). The film formed in TMAP/GBL containing 0.01 wt% of water (Fig. 29d) composed of fibrils and a barrier layer, which were a dehydrated aluminum oxide (O/Al = 1.0 - 2.0, C/Al = 0 - 0.08).

(d) AES

AES showed that the film formed in TEMAM/GBL (Fig. 30a and 30b) was thinner than those formed in TMAP/GBL (Fig. 30c and 30d). The films formed in TMAP/GBL containing 0.01 wt% (Fig. 30d) were thicker than those formed in TMAP/GBL containing 1 wt% (Fig. 30c) due to its porous-type structure. The phthalate anion was slightly incorporated only on the surface.

High carbon content from the bottom of the film to its surface in Fig. 30b indicates that maleate anion was utilized as an oxygen source instead of water at nearly anhydrous condition. The

concentration of carbon atom may be overestimated because of the difference between the carbon atom in the composite aluminum oxide and that in a standard graphite.

(e) Chemical Analysis

Elemental analysis of the isolated films by iodine-methanol treatment revealed the carbon content in the films formed in TEMAM/GBL and TMAP/GBL were about 20 and 6 wt%, respectively. The isolated film formed in the maleate solution was dissolved in sulfuric acid. Maleic acid and unknown derivatives were detected from this solution by liquid chromatography as shown in Fig. 31.

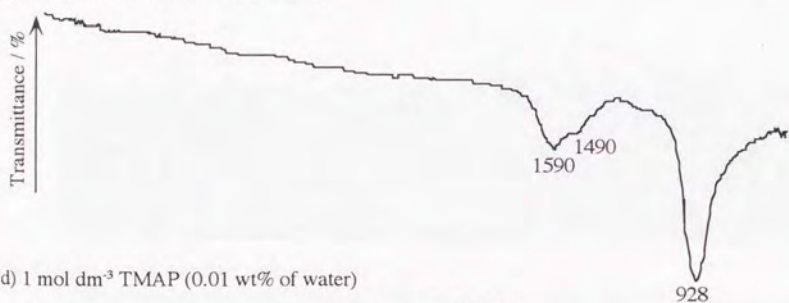
(a) 1 mol dm^{-3} TEMAM (1 wt% of water)



(b) 1 mol dm^{-3} TEMAM (0.01 wt% of water)



(c) 1 mol dm^{-3} TMAP (1 wt% of water)



(d) 1 mol dm^{-3} TMAP (0.01 wt% of water)

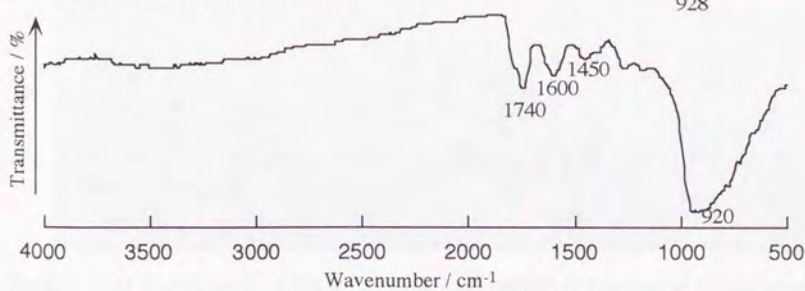


Fig. 27. FT-IR spectra of the anodic films formed in TEMAM/GBL and TMAP/GBL.

(a) 1 mol dm^{-3} TEMAM (1 wt% of water)



(b) 1 mol dm^{-3} TEMAM (0.01 wt% of water)



(c) 1 mol dm^{-3} TMAP (1 wt% of water)

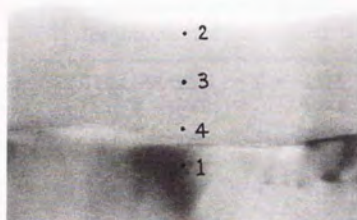


(d) 1 mol dm^{-3} TMAP (0.01 wt% of water)

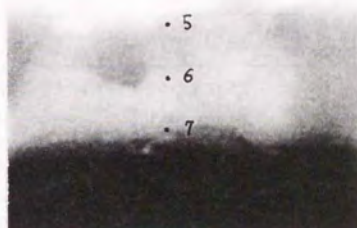


Fig. 28. TEM micrographs of the ultramicrotomed section of the anodic films formed in TEMAM/GBL and TMAP/GBL.

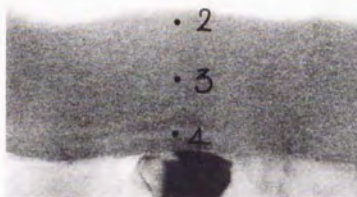
(a) 1 mol dm^{-3} TEMAM (1 wt% of water)



(b) 1 mol dm^{-3} TEMAM (0.01 wt% of water)



(c) 1 mol dm^{-3} TMAP (1 wt% of water)



100 nm

(d) 1 mol dm^{-3} TMAP (0.01 wt% of water)

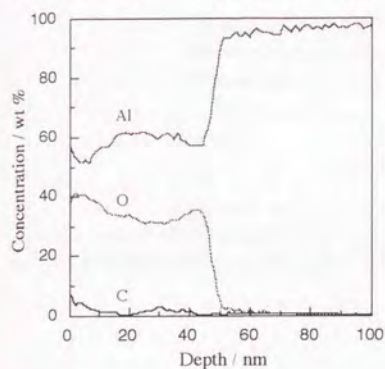


Fig. 29. STEM micrographs of the ultramicrotomed section of the anodic films formed in TEMAM/GBL and TMAP/GBL. The nominal positions for EDX are indicated.

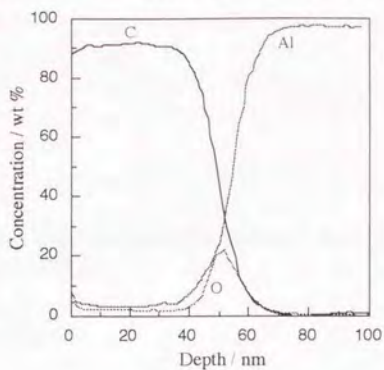
Table 17. X-ray counts from the stationary probe positions indicated in Fig. 27 and calculated atomic ratios.

| Electrolyte | | O | Al | C | O/Al | C/Al |
|-------------------------------|---|------|------|------|------|------|
| TEMAM/GBL (1 wt% water) | 2 | 1526 | 1038 | 124 | 2.34 | 0.32 |
| | | 1734 | 894 | 87 | 3.09 | 0.26 |
| | 3 | 2340 | 1351 | 184 | 2.76 | 0.36 |
| | | 1996 | 1441 | 124 | 2.21 | 0.23 |
| | 4 | 2755 | 1583 | 115 | 2.77 | 0.19 |
| | | 2280 | 1560 | 110 | 2.33 | 0.19 |
| TEMAM/GBL (0.01 wt% water) | 5 | 597 | 509 | 896 | 1.87 | 4.67 |
| | | 658 | 872 | 834 | 1.20 | 2.54 |
| | 6 | 618 | 812 | 748 | 1.21 | 2.44 |
| | | 582 | 688 | 1134 | 1.35 | 4.37 |
| | 7 | 578 | 720 | 776 | 1.28 | 2.86 |
| | | 548 | 656 | 1830 | 1.33 | 7.40 |
| TMAP/GBL (1 wt% water) | 2 | 677 | 530 | 9.5 | 2.04 | 0.05 |
| | | 561 | 206 | 15.5 | 4.34 | 0.20 |
| | 3 | 767 | 740 | 8.0 | 1.65 | 0.03 |
| | | 618 | 255 | 15.5 | 3.86 | 0.16 |
| | 4 | 669 | 663 | 6.0 | 1.61 | 0.02 |
| | | 651 | 430 | 11.0 | 2.41 | 0.07 |
| TMAP/GBL (0.01 wt% water) | 5 | 333 | 442 | 13.5 | 1.20 | 0.08 |
| | | 401 | 589 | 17.5 | 1.09 | 0.08 |
| | 6 | 366 | 295 | 8.0 | 1.98 | 0.07 |
| | | 346 | 435 | 8.5 | 1.27 | 0.05 |
| | 7 | 607 | 697 | 0.5 | 1.39 | 0.00 |
| | | 525 | 667 | 0.0 | 1.25 | 0.00 |

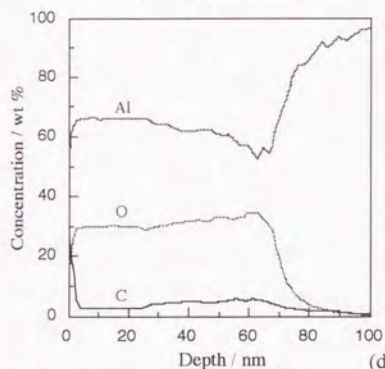
(a) 1 mol dm⁻³ TEMAM (1 wt% of water)



(b) 1 mol dm⁻³ TEMAM (0.01 wt% of water)



(c) 1 mol dm⁻³ TMAP (1 wt% of water)



Sputtering rate = 5 nm min⁻¹ for SiO₂.

(d) 1 mol dm⁻³ TMAP (0.01 wt% of water)

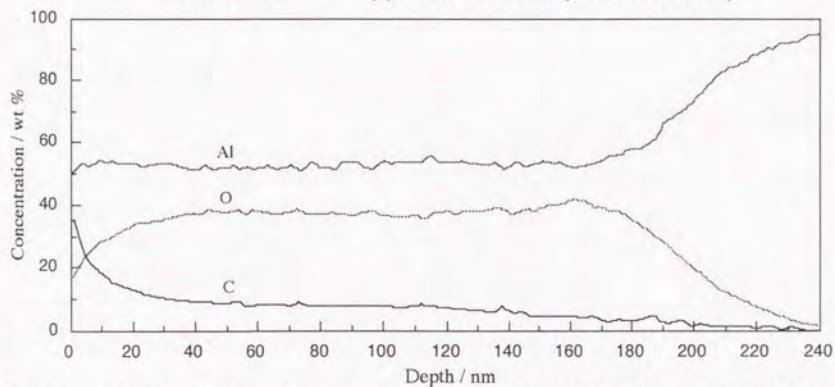


Fig. 30. AES depth profiles of the anodic films formed in TEMAM/GBL and TMAP/GBL.

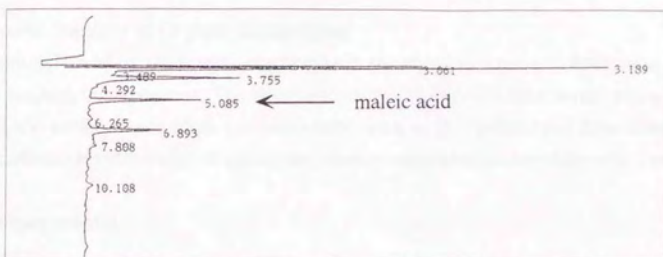


Fig. 31. Liquid chromatogram of the solution that comprised the dissolved anodic film formed in TEMAM/GBL containing 0.01 wt% of water.

2.8. Chemical Stability of Organic Electrolytes

The chemical stability of organic electrolyte is an important factor to determine the life of aluminum electrolytic capacitors. The deterioration mechanisms for ammonium adipate/ethylene glycol [66] and tertiary ammonium maleate/ γ -butyrolactone [67] electrolytes have been reported.

The deterioration mechanism of quaternary ammonium carboxylate/ γ -butyrolactone has been examined.

2.8.1. Experimental

Electrolyte

Three kinds of 25 wt% - quaternary ammonium carboxylate/ γ -butyrolactone electrolytes (Mitsubishi Petrochemical Co.) were used. The following abbreviations were used for solutes and solvent: triethylmethylammonium hydrogen maleate (TEMAM), tetramethylammonium hydrogen phthalate (TMAP), triethylmethylammonium benzoate (TEMAB) and γ -butyrolactone (GBL).

Procedures

These electrolytes were filled in 100 ml liquefied gas sampling tube (Taiatsu Scientific Glass Co., A-2). These tubes were placed in an oven. Each deteriorated electrolyte was sampled after regular intervals and their electrolytic conductivities were measured at 25°C by a conductivity meter equipped with a standard type conductivity cell (Toa Electronics, CM-60S/CGT-511B).

For quantitative analysis of decomposed products, a 200 ml portable reactor (Taiatsu Scientific Glass, Co., TVS) or 1 l gas sampling bottle (GL Science Co.) was used. After a given time, gas and liquid phase of the deteriorated electrolytes were analyzed by a gas chromatography (Perkin-Elmer, Σ 2000), liquid chromatography (Waters, Model 510) and gel chromatography (Shimadzu, LC-6AD).

2.8.2. Results and Discussion

The changes in electrolytic conductivity of the deteriorated electrolytes at 115°C are given in Fig. 32. As discussed in Chap. 2.3, the phthalate solution showed excellent stability, while the maleate and benzoate solutions deteriorated with time. Particularly, the electrolytic conductivity of the benzoate solution fell rapidly within 100 hr and then decreased gradually. In order to clarify the decomposition mechanisms, the decomposition products were analyzed quantitatively.

Fig. 33 shows the mass balance of the benzoate salt. This result verified the decomposition mechanism shown in Fig. 34.

In Fig. 35, the decrease in maleic acid content strongly correlates with the decrease in electrolytic conductivity in Fig. 32. However, the decomposition rate was not so large as the benzoate, the reaction temperature was raised to 150°C. The formation of carbon dioxide was parallel to the loss of maleic acid as shown in Fig. 36. The decarboxylation of maleic acid is a main reaction followed by the formation of polymeric unknown compounds shown in Fig. 37.

The difference in chemical stability between the phthalate and benzoate solution can be ascribed to the difference in ionic dissociation as indicated in Chap. 2.4. That is, ion formation accelerates the decomposition reaction according to the reaction scheme shown in Fig. 38.

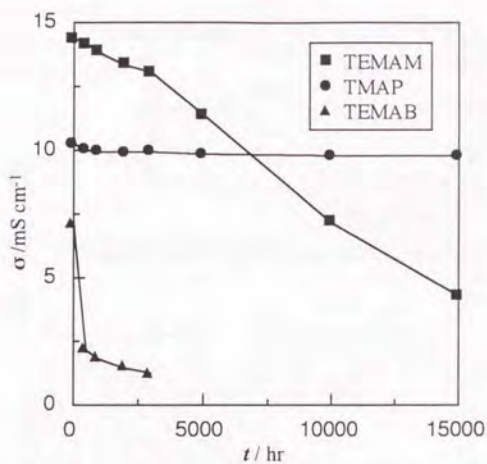


Fig. 32. Deterioration of electrolytic conductivity of the electrolytes at 115°C.

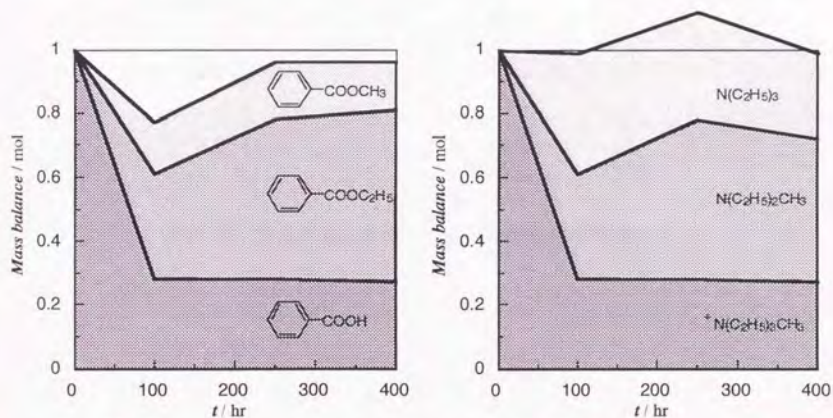


Fig. 33. Mass balance of decomposition products of the benzoate solution.

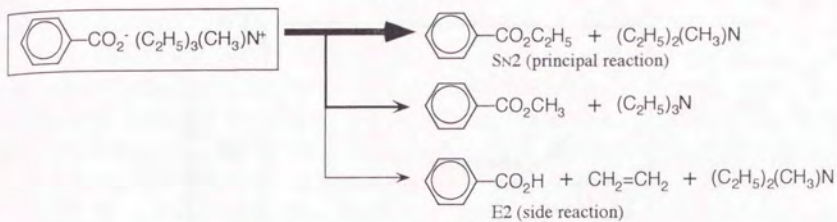


Fig. 34. Decomposition mechanisms for the benzoate salt.

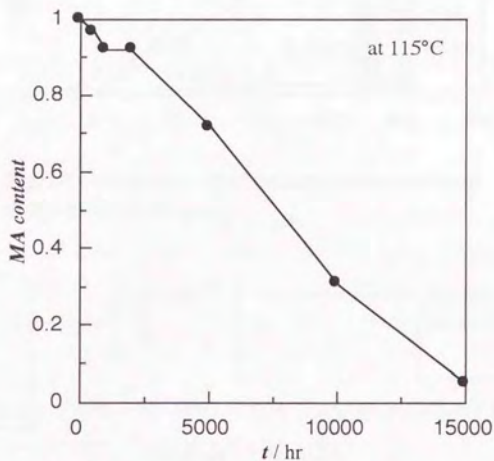


Fig. 35. Decrease of maleic acid content with time.

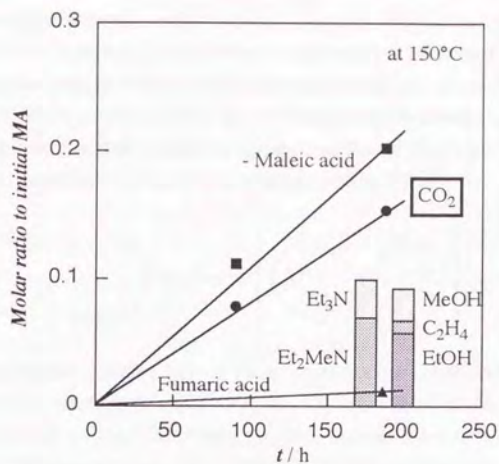


Fig. 36. Mass balance of decomposition products of the maleate solution.

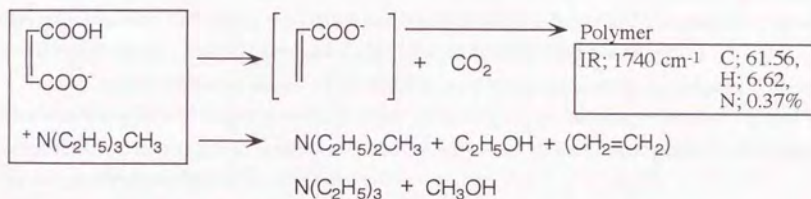


Fig. 37. Decomposition mechanisms for the maleate salt.

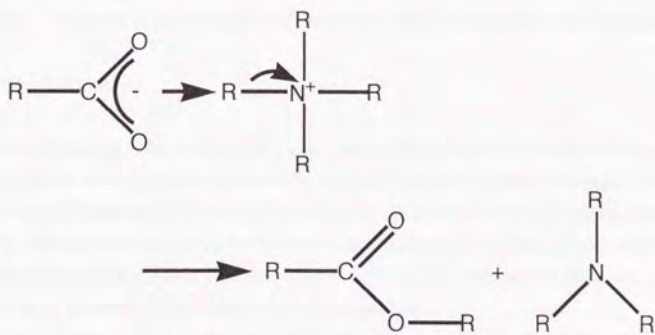
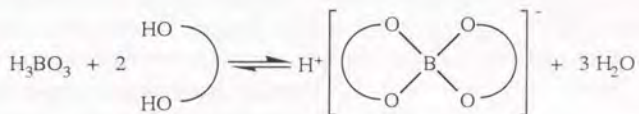


Fig. 38. Proposed decomposition mechanism.

2.9. Organo-Boron Complexes

The reaction of boric acid with polyhydroxy compounds has been used for many years as a means of increasing the strength of boric acid for its titration, and also as a means of characterizing carbohydrates [68]. Boric acid forms the four-coordinated chelate anionic complexes containing a tetrahedral BO_4 unit with polyols, hydroxycarboxylic acids and dicarboxylic acids, which have *cis*-hydroxy groups according to the following reaction scheme [67].



Alkali metal, ammonium or amine salts of these complexes have been used as the solute in the electrolyte of aluminum electrolytic capacitors [68 - 72], however, their quaternary ammonium salts have been reported only for those with aromatic ligands such as borodisalicylate [68], borodinaphthoates [68], borodicatcholates [68, 73], borodinaphthalenediolates [68, 73] and borodibiphenolate [73].

In order to find highly conductive electrolytes for low-impedance capacitors based on the quaternary ammonium salt/ γ -butyrolactone electrolyte systems, preparation of the quaternary ammonium salts of the borate complexes having smaller ligands has been attempted. Among several tested ligands, glycolic acid and oxalic acid afforded the stable compounds.

Preparation and characterization of these new quaternary ammonium borodiglycolate and borodioxalate salts will be presented. Stability of the organo-boron complexes is discussed by examining the enhancement in conductivity and acidity caused by the complexation between boric acid and polyhydroxy ligands in water and γ -butyrolactone.

The electrochemical properties such as ionization constant, conductivity, limiting molar conductivity, ion association constant, oxidation potential and film forming ability of anodic aluminum oxide are given for these quaternary ammonium borodiglycolate and borodioxalate in γ -butyrolactone. The results are compared with those of the borodisalicylate and borodicatcholate salts.

2.9.1. Experimental

Reagents

Guaranteed-grade boric acid, oxalic acid, succinic acid, salicylic acid (Wako Pure Chemical Industries), glycolic acid, malonic acid, maleic acid and catechol (Tokyo Chemical Industry Co.) were used without further purification. Ultrapure-grade 25 wt % tetramethylammonium hydroxide and 40 wt % tetraethylammonium hydroxide aqueous solutions (SACHEM Inc.) as well as battery-grade γ -butyrolactone (Mitsubishi Petrochemical Co., F-GBL) were used as received.

Preparation of quaternary ammonium tetrahydroxyborates

Into a tetraethylammonium hydroxide aqueous solution, an equimolar boric acid was added. The water was evaporated at 50°C and the resultant white solid was dried *in vacuo* at 80°C to give tetraethylammonium tetrahydroxyborate.

Elemental analysis: Calcd. for $C_8H_{24}NBO_4$: C, 45.96; H, 11.57; N, 6.70; B, 5.17. Found: C, 45.60; H, 11.18; N, 6.89; B, 5.47.

^{11}B -n.m.r. (in D_2O): -14.6 ppm relative to H_3BO_3 in water as $\delta = 0.0$ ppm.

XPS: B_{1s} , 191.7; C_{1s} , 284.6, 286.5; N_{1s} , 401.6, 398.7; O_{1s} , 531.5 eV.

Preparation of quaternary ammonium organo-boron complexes

Into an equimolar aqueous solution of tetramethylammonium or tetraethylammonium hydroxide and boric acid (*in situ* preparation of tetrahydroxyborate), two equivalents of glycolic acid or oxalic acid was added. The water was removed by evaporation at $50^\circ C$ and the resultant white solid was recrystallized from 2-propanol (methanol for tetramethylammonium borodioxalate) and then dried *in vacuo* at $80^\circ C$.

(1) Tetramethylammonium borodiglycolate

Elemental analysis: Calcd. for $C_8H_{16}NBO_6$: C, 41.23; H, 6.92; N, 6.01; B, 4.64. Found: C, 41.44; H, 6.73; N, 5.95; B, 4.67.

n.m.r. (D_2O) in ppm: 1H , 3.2 (N- CH_3), 4.3 (O- CH_2 - CO_2); ^{11}B , -8.2; ^{13}C , 57.9 (N- CH_3), 63.0 (O- CH_2 - CO_2), 180.6 (O- CH_2 - CO_2).

(2) Tetraethylammonium borodiglycolate

Elemental analysis: Calcd. for $C_{12}H_{24}NBO_6$: C, 49.85; H, 8.37; N, 4.84; B, 3.74. Found: C, 49.62; H, 8.27; N, 4.85; B, 3.78.

n.m.r. (D_2O) in ppm: 1H , 1.3 (N- CH_2 - CH_3), 3.2 (N- CH_2 - CH_3), 4.3 (O- CH_2 - CO_2); ^{11}B , -8.2; ^{13}C , 9.2 (N- CH_2 - CH_3), 54.6 (N- CH_2 - CH_3), 63.0 (O- CH_2 - CO_2), 180.6 (O- CH_2 - CO_2).

(3) Tetramethylammonium borodioxalate

Elemental analysis: Calcd. for $C_8H_{12}NBO_8$: C, 36.82; H, 4.63; N, 5.37; B, 4.14. Found: C, 37.10; H, 4.40; N, 5.45; B, 4.26.

n.m.r. (D_2O) in ppm: 1H , 3.2 (N- CH_3); ^{11}B , -11.7; ^{13}C , 58.0 (N- CH_3), 165.3 ($-CO_2$ -).

(4) Tetraethylammonium borodioxalate

Elemental analysis: Calcd. for $C_{12}H_{20}NBO_8$: C, 45.45; H, 6.36; N, 4.42; B, 3.41. Found: C, 45.57; H, 6.18; N, 4.45; B, 3.57.

n.m.r. (D_2O) in ppm: 1H , 1.3 (N- CH_2 - CH_3), 3.2 (N- CH_2 - CH_3); ^{11}B , -11.7; ^{13}C , 9.2 (N- CH_2 - CH_3), 54.6 (N- CH_2 - CH_3), 166.2 ($-CO_2$ -).

(5) Other salts

Tetramethylammonium and tetraethylammonium borodisalicylates and borodiccatecholates were synthesized in a similar manner to that described in the literature [69, 74].

Electrochemical apparatus

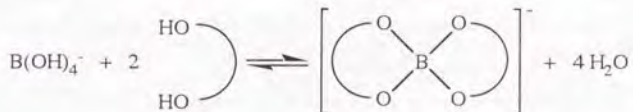
The conductivity and acidity were measured by a conductivity meter/standard type conductivity cell (Toa Electronics, CM-60S/CGT-511B) and a pH meter/composite glass electrode (Toa Electronics, HM-11P/GST-2411C), respectively. The water content in γ -butyrolactone solution was measured by a moisture meter (Mitsubishi Kasei Co., CA-06). The acidity of γ -butyrolactone solution was measured in an argon glove box by monitoring potential difference between a glass electrode (Toa Electronics, order-made) and a double junction $Pt/I_3^-/I^-$ reference electrode [74] on an intelligent recorder (Toa Electronics, INR-6061). Oxidation potential was measured by an

automatic polarization system (Hokuto Denko Co., HZ-1A). The conductometric analysis and aluminum anodization and were carried out by the methods previously described (See Chap. 2.4 and 2.6).

2.9.2. Results and Discussion

Preparation of quaternary ammonium organo-boron complexes

Investigations using a variety of techniques have established that the complexation with the polyhydroxy ligands is much more pronounced when the tetrahydroxyborate ion, $B(OH)_4^-$, is used instead of boric acid itself as shown in the following equation [69, 75].



Similar to alkali metal or alkaline earth metal salts of tetrahydroxyborate [76-78], tetraethylammonium tetrahydroxyborate was isolated by removing water from the reaction mixture of tetraethylammonium hydroxide and boric acid. The ^{11}B -n.m.r. spectrum of this salt in D_2O showed a sharp peak at $\delta = -14.6$ ppm. The tetrahedral $B(OH)_4^-$ species have been identified as a sharp signal at -17 ppm in aqueous solutions [79].

The reaction of tetramethylammonium or tetraethylammonium tetrahydroxyborate with two equivalents of ligands gave tetramethylammonium or tetraethylammonium organo-boron complexes. As a ligand, glycolic acid, oxalic acid, salicylic acid and catechol afforded stable complexes.

On the other hand, we have failed to isolate complexes with malonic acid, succinic acid or maleic acid under the same condition, although amine salts of organo-boron complex with malonic acid were prepared by azeotropic removal of water [80].

Stability of organo-boron complexes

To examine the stability of organo-boron complexes, the enhancements in conductivity and acidity by the complexation were examined.

Conductivity results are given in Table 18 both for aqueous and γ -butyrolactone solutions, where σ_L is the conductivity of 0.1 mol dm^{-3} ligand solution (L) and σ_M is the conductivity of 0.05 mol dm^{-3} boric acid plus 0.1 mol dm^{-3} ligand mixture solution (M). Δ_c is conductivity increment, which is the conductivity of M minus the sum of the conductivities of the individual L and boric acid solutions. It is evident from Table 18 that glycolic acid, oxalic acid and salicylic acid can form organo-boron complexes, while succinic acid and maleic acid cannot. The positive conductivity increment in γ -butyrolactone for malonic acid remains a possibility for forming the complex in non-aqueous solvents. This agrees with the result that borodimalonate can be isolated under anhydrous conditions [80].

Acidity increase was not observed by an ordinary pH measurement for any aqueous solutions used for the conductivity experiment. However, pH measurement of the γ -butyrolactone solutions showed remarkable enhancement of proton activity as shown in Table 19, where E_L and E_M are

potentials (mV vs. I_3^-/I^- at 30°C) of solution L and M, respectively (pK_f values of ligand in water [81] are given for reference to validate the E_L values.). Δ_E is the potential increment $E_L - E_M$, where 60 mV corresponds to 1 pH unit by Nernst equation. Although the potential increase in Table 19 includes the effect of water increase (from ca. 100 to ca. 2400 ppm) besides that of the complexation, these data are also useful as a criterion of the complexation.

Table 18. Effect of ligand on conductivity of boric acid in water and GBL at 25°C.

| Ligand | in H ₂ O | | | in GBL | | |
|----------------|---------------------|------------|------------|------------|------------|------------|
| | σ_L | σ_M | Δ_C | σ_L | σ_M | Δ_C |
| None | - | 10 | - | - | 1.1 | - |
| Glycolic acid | 1546 | 1575 | 19 | 1.5 | 16.9 | 14.3 |
| Oxalic acid | 21900 | 22300 | 390 | 3.2 | 772.0 | 767.7 |
| Malonic acid | 4670 | 4660 | -20 | 7.3 | 11.9 | 3.5 |
| Succinic acid | 952 | 946 | -16 | 0.4 | 0.6 | -0.9 |
| Maleic acid | 12190 | 12090 | -110 | 1.0 | 1.3 | -0.8 |
| Salicylic acid | - | - | - | 0.6 | 128.0 | 126.3 |

in $\mu\text{S cm}^{-1}$

Table 19. Effect of ligand on acidity of boric acid in GBL at 30°C.

| Ligand | pK_f (in H ₂ O) | H ₂ O / ppm | | E_L | E_M | Δ_E |
|----------------|---------------------------------|------------------------|------|-------|-------|------------|
| | | L | M | | | |
| None | - | 30 | 2470 | - | 141 | - |
| Glycolic acid | 3.82 | 120 | 2350 | 28 | 429 | 401 |
| Oxalic acid | 1.27 | 70 | 2320 | 283 | 548 | 265 |
| Malonic acid | 2.86 | 140 | 2380 | 145 | 408 | 263 |
| Succinic acid | 4.21 | 100 | 2530 | 30 | 217 | 187 |
| Maleic acid | 1.94 | 80 | 2450 | 86 | 316 | 230 |
| Salicylic acid | 3.00 | 100 | 2260 | 161 | 504 | 343 |

/ mV vs. I_3^-/I^-

Ionization constant

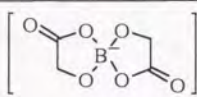
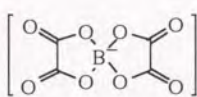
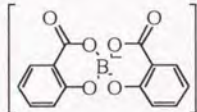
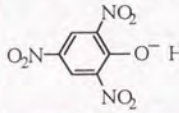
Ionization constants of the conjugated acids of borodiglycolate, borodioxalate and borodisalicylate in γ -butyrolactone were first determined by potentiometric measurement of 5×10^{-3} mol dm⁻³ equimolar acid-base mixtures (proton form/tetramethylammonium form) at 30°C. Observed potentials E (mV vs. I₃⁻/I⁻) were calibrated by 5×10^{-3} mol dm⁻³ picric acid/tetraethylammonium picrate γ -butyrolactone buffer solution using $pK_a = 7.26$ [22] as shown in Table 20. It is remarkable that organo-boron complexes are fairly strong acids, particularly the acidity of borodioxalate complex is comparable with that of trifluoromethanesulfonic acid [74].

Molar conductivity

Conductivities of quaternary ammonium organo-boron complex/ γ -butyrolactone electrolytes were measured at a practical concentration of 1 mol dm⁻³ at 25°C. Tetramethylammonium borodiglycolate and borodioxalate showed higher conductivities than borodisalicylate and borodicaticholate reflecting their stronger acidities and smaller ion sizes as shown in Table 21.

Higher conductivities of tetramethylammonium salts than tetraethylammonium counterparts indicate a higher dissociation tendency of organo-boron complexes compared to weak carboxylic acids, because the conductivities of tetramethylammonium carboxylates are lower than those of tetraethylammonium carboxylates owing to ion association (See Chap. 2.4).

Table 20. Observed potentials and ionization constants of organo-boron complexes in GBL at 30°C.

| Organo-boron complex | E / mV vs. I ₃ ⁻ /I ⁻ | pK_a |
|-------------------------------------------------------------------------------------|-------------------------------------------------------------|--------|
|  | H ⁺ 270 | 6.0 |
|  | H ⁺ 507 | 2.1 |
|  | H ⁺ 411 | 3.7 |
|  | 196 | 7.26* |
| (standard for calibration) | | |

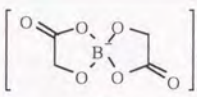
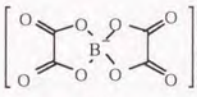
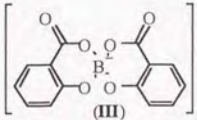
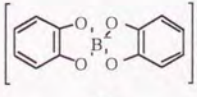
* Ref. 22.

The molar conductivities of tetramethylammonium organo-boron complexes were obtained over the molar concentration range of 10^{-2} to 10^{-3} mol dm $^{-3}$ as shown in Table 22.

Table 21. Molar conductivities of 1 mol dm $^{-3}$ quaternary ammonium organo-boron complex/GBL electrolytes at 25°C.

| Organo-boron complex | Me $_4$ N $^+$ | Et $_4$ N $^+$ |
|----------------------|----------------|----------------|
| Borodiglycolate | 10.76 | 10.48 |
| Borodioxalate | 11.15 | - |
| Borodisalcilate | 6.46 | 5.42 |
| Borodicatcolate | 6.66 | - |

Table 22. Molar concentrations and molar conductivities of tetramethylammonium organo-boron complexes in GBL at 25°C.

| Organo-boron complex | $10^3 C$ / mol dm $^{-3}$ | Λ / S cm 2 mol $^{-1}$ |
|----------------------------------------------------------------------------------------------|------------------------------|--------------------------------------|
|  (I) | 9.9215 | 34.980 |
| | 7.4417 | 35.697 |
| | 4.9572 | 36.765 |
| | 2.4802 | 38.283 |
| | 1.7380 | 38.953 |
| | 0.9942 | 39.578 |
|  (II) | 9.4627 | 35.175 |
| | 7.0953 | 35.833 |
| | 4.7384 | 36.774 |
| | 2.3685 | 38.231 |
| | 1.6572 | 38.711 |
| | 0.9480 | 39.398 |
|  (III) | 9.3602 | 29.663 |
| | 7.0174 | 30.332 |
| | 4.6847 | 31.197 |
| | 2.3399 | 32.544 |
| | 1.6420 | 33.234 |
| | 0.9641 | 33.648 |
|  (IV) | 9.9926 | 31.638 |
| | 7.4940 | 32.379 |
| | 4.9945 | 33.407 |
| | 2.4993 | 34.910 |
| | 1.7534 | 35.417 |
| | 0.9941 | 36.092 |

Analysis of conductivity data

The conductivity data were analyzed by means of the Fernández-Prini expansion of the Fuoss-Hsia equation (See Chap. 6).

Derived limiting molar conductivities Λ_0 and ion association constants K_A are given in Table 23 as well as single ion limiting molar conductivities λ_0^- , which are obtained by subtracting the single ion limiting molar conductivity of tetramethylammonium ($\lambda_0^+ = 21.5 \text{ S cm}^2 \text{ mol}^{-1}$; See Chap. 4.3) from the limiting molar conductivities. Standard deviations in Λ_0 and K_A were less than 0.03 and 0.2, respectively. The ionic radii r estimated from MNDO calculation are also given in Table 23.

Walden products of all organo-boron complex anions almost follow the theoretical behavior, which suggest that they are able to move without adhesion to γ -butyrolactone as most anions do (See Cap. 2.4). These results clearly indicate that higher conductivities of borodiglycolate and borodioxalate than borodisalicylate and borodiccatecholate can be attributed to their smaller ion size without aromatic rings.

Derived ion association constants of the organo-boron complexes are smaller than those of the free carboxylic acids due to their stronger acidity and their magnitude is closely related to the pK_a values given in Table 20.

Table 23. Limiting molar conductivities, ion association constants and single ion limiting molar conductivities of organo-boron complexes in GBL at 25°C and estimated ionic radii.

| Complex | Λ_0 / $\text{S cm}^2 \text{ mol}^{-1}$ | K_A / $\text{dm}^3 \text{ mol}^{-1}$ | λ_0^- / $\text{S cm}^2 \text{ mol}^{-1}$ | r / nm |
|---------|---------------------------------------------------|-------------------------------------------|-----------------------------------------------------|-------------|
| I | 41.63 | 9.2 | 20.1 | 0.289 |
| II | 41.98 | 11.3 | 20.5 | 0.283 |
| III | 35.86 | 11.1 | 14.3 | 0.362 |
| IV | 38.41 | 11.9 | 16.9 | 0.340 |

Anodic oxidation of aluminum

The electrolyte of aluminum electrolytic capacitors requires the ability to produce an aluminum oxide film on aluminum anode when it is electrochemically oxidized in the electrolyte. It is well known that monobasic acids have poor film forming ability because of their corrosive property (anodic dissolution of aluminum) [9]. Therefore, the organo-boron complexes are thought to fall in this category from this point of view.

The film forming ability of the organo-boron complexes was examined by galvanostatic anodization of high purity aluminum foil in 1 mol dm^{-3} tetramethylammonium organo-boron complex/ γ -butyrolactone solution containing about 500 ppm of water at 0.5 A dm^{-2} . The change in formation voltage V_f with time t is given in Fig. 39.

Borodiglycolate (I) and borodioxalate (II) gave saturated curves, which are the indications both anodic dissolution and oxidation occurred, simultaneously. The maximum voltages attained were about one-fourth of those of glycolate and oxalate [82]. This is presumably caused by the strong acidity of organo-boron complexes. On the other hand, borodisalicylate (III) showed a favorable upward curve up to scintillation around 90 V, which is almost the same as that of salicylate salt [5]. Borodicatatecholol (IV) decomposed during anodization and the color of the electrolyte turned to black.

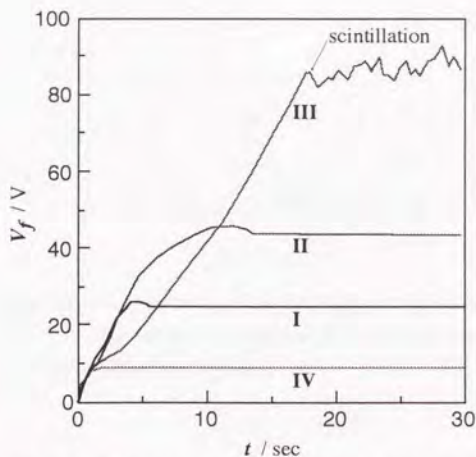


Fig. 39. Anodization of aluminum in 1 mol dm^{-3} tetramethylammonium organo-boron complex/ γ -butyrolactone electrolytes.

Oxidation potential

The electrolyte of aluminum electrolytic capacitors does not need severe durability against oxidation or reduction like those of electrical double layer capacitors or lithium batteries, because the applied voltage is not sustained by the electrolyte itself but aluminum oxide. However, the stability toward oxidation is more or less necessary.

Oxidation potentials of organo-boron complexes were measured by scanning the potential of platinum electrode relative to $\text{Pt}/\text{I}_3^-/\text{I}^-$ reference electrode at 50 mV s^{-1} rate. Polarization curves are given in Fig. 40.

Borodiglycolate (I) and borodioxalate (II) began to decompose around 1.5 V, more positive than borodisalicylate (III) and borodiccatecholate (IV) due to lack of aromatic rings. Borodiccatecholate (IV) was very unstable to oxidation, which was observed in anodization of aluminum.

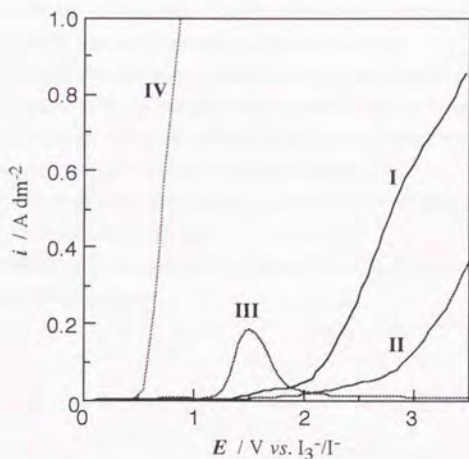


Fig. 40. Oxidation potentials on platinum electrode in 1 mol dm^{-3} tetramethylammonium organo-boron complex/GBL electrolytes.

2.10. Summary

An organic electrolyte consisting of quaternary ammonium carboxylate salts and γ -butyrolactone solvent has acquired a potential application for aluminum electrolytic capacitors. The high electrolytic conductivity and chemical stability of the new electrolyte were demonstrated in comparison with traditional electrolytes.

Conductometric analysis has revealed that quaternary ammonium carboxylates are significantly dissociated in γ -butyrolactone solvent to show high electrolytic conductivities, whereas tertiary ammonium carboxylates are strongly associated in the solvent due to hydrogen bond effect.

The film forming ability in anodic oxidation of aluminum of the quaternary ammonium carboxylate/ γ -butyrolactone electrolyte was almost the same as the tertiary ammonium counterpart except for its lower scintillation voltage. The film forming ability of the electrolyte depended entirely on the kind of carboxylate anion, its concentration and the amount of water. Maleate solution showed fast and efficient film formation and resulted in a barrier-type oxide film regardless of the water content. On the other hand, phthalate and benzoate solution afforded both barrier and porous-type oxide layers depending on the water content.

The anodic films formed under nearly anhydrous condition proved to be entirely new films. The fibrous-type film was created in the phthalate solution containing less water accompanied by the decomposition of the electrolyte. The first deep and heavy anion uptake was found in the maleate solution containing less water to give a composite aluminum oxide.

The chemical stability of the solutes was also correlated with ion pair formation in solution, which accelerates the decomposition reaction.

Finally, electrochemical properties of new quaternary ammonium organo-boron complexes were introduced for capacitor application.

2.11. References

1. W. J. Bernard, *J. Electrochem. Soc.*, **124**, 403C (1977)
2. J. Barthel, H. J. Gores, G. Schmeer and R. Wachter, "Non-Aqueous Electrolyte Solutions in Chemistry and Modern Technology", *Topics in Current Chemistry*, **111**, 33 (1983).
3. Izaya Nagata, *Aluminum Dry Electrolytic Capacitors*, Japan Capacitor Ind., Tokyo (1983).
4. M. Ue, K. Ida and S. Mori, *Chemitopia*, **12**, 2 (1993).
5. M. Ue, *TCSC News Letters*, **23**, 89 (1993).
6. M. Ue and S. Mori, *Electrolytic Condenser Review*, **45**, 1 (1994).
7. S. Mori and M. Ue, *USP* 4715976 (1987); *JP* 91-6646B, 8092B (1991); *EP* 227433B (1992).
8. S. Mori, K. Ida and M. Ue, *USP* 4892944 (1990).
9. S. Tajima, S. Itoh and T. Fukushima, *Denki Kagaku*, **23**, 296 (1955).
10. S. Tajima, S. Itoh and T. Fukushima, *Denki Kagaku*, **23**, 342 (1955).
11. S. Tajima, S. Itoh and T. Fukushima, *Denki Kagaku*, **23**, 395 (1955).
12. I. M. Kolthoff and M. K. Chantooni, Jr., *J. Amer. Chem. Soc.*, **85**, 426 (1963).
13. I. M. Kolthoff and M. K. Chantooni, Jr., *J. Phys. Chem.*, **70**, 856 (1966).
14. I. M. Kolthoff and M. K. Chantooni, Jr., *J. Amer. Chem. Soc.*, **97**, 1376 (1975).
15. I. M. Kolthoff, M. K. Chantooni, Jr. and H. Smagowski, *Anal. Chem.*, **42**, 1622 (1970).
16. E. Roletto, A. Vanni and V. Zelano, *Ann. Chimica*, **70**, 147 (1980).
17. E. Roletto, A. Vanni and V. Zelano, *Ann. Chimica*, **70**, 375 (1980).
18. Z. Pawlak, R. A. Robinson and R. G. Bates, *J. Solution Chem.*, **7**, 631 (1978).
19. M. L. Jansen and H. L. Yeager, *J. Phys. Chem.*, **77**, 3089 (1973).
20. M. Ue, unpublished results.
21. K. Izutsu, *Acid-Base Dissociation Constants in Dipolar Aprotic Solvents*, *IUPAC Chemical Data Series No. 35*, Blackwell Scientific, Oxford (1990).
22. K. Izutsu, T. Nakamura and H. Suzuki, *41st Annual Meeting of the Japan Society for Analytical Chemistry*, Abstract, p. 336 (1992).
23. A. I. Shcherban, I. V. Perevertkina and G. V. Kharitonov, *Zh. Obshch. Khim.*, **58**, 270 (1988).
24. A. I. Shcherban, I. V. Perevertkina and G. V. Kharitonov, *Zh. Obshch. Khim.*, **58**, 273 (1988).
25. N. Baba, *Kinzoku Hyomen Gijutsu*, **25**, 609 (1974).
26. J. M. Kape, *Plating*, **26** (1968).
27. D. R. Clarke, D. W. Hamilton and T. R. Beck, *Plating*, 1342 (1967).
28. N. Kanzaki, R. Shimatani, H. Takahashi and H. Tokumasu, *Hyomen Gijutsu*, **41**, 808 (1990).
29. S. Tajima, N. Baba and T. Mori, *Electrochim. Acta*, **9**, 1509 (1964).
30. G. C. Wood and G. W. Patrick, *Trans. Inst. Metal Finishing*, **45**, 174 (1967).
31. T. Yoshino and N. Baba, *Kinzoku Hyomen Gijutsu*, **23**, 375 (1972).
32. H. Nakata, *Electrolytic Condenser Review*, **38**, 21 (1970).

33. S. Ikonopisov, A. Girginov and M. Machkova, *Electrochim. Acta*, **22**, 1283 (1977).
34. S. Ikonopisov, N. Elenkov, E. Klein and L. Andreeva, *Electrochim. Acta*, **23**, 1209 (1978).
35. S. Ikonopisov, A. Girginov and M. Machkova, *Electrochim. Acta*, **24**, 451 (1979).
36. S. Morisaki, N. Baba and S. Tajima, *Denki Kagaku*, **38**, 443 (1970).
37. T. Nishiyama and R. Kojima, *Denki Kagaku*, **41**, 633 (1973).
38. R. S. Alwitt and R. G. Hills, *J. Electrochem. Soc.*, **112**, 974 (1965).
39. R. W. Santway and R. S. Alwitt, *J. Electrochem. Soc.*, **117**, 1282 (1970).
40. K. Shimizu, G. E. Thompson and G. C. Wood, *Thin Solid Films*, **85**, 53 (1981).
41. Y. Nitta, M. Morita and Y. Matsuda, *Denki Kagaku*, **58**, 74 (1990).
42. D. J. Sharp, J. K. G. Panitz, R. M. Merrill and D. M. Haaland, *Thin Solid Films*, **111**, 227 (1984).
43. L. Campanella, *Plating*, **57** (1969).
44. L. Campanella, *Plating*, **47** (1971).
45. M. D. Rausch, W. McEwen and J. Kleinberg, *J. Amer. Chem. Soc.*, **77**, 2093 (1955).
46. K. Matsuki, M. Sugawara and A. Sawaguchi, *1991 Fall Meeting of the Electrochemical Society of Japan*, Abstract, p. 170 (1991).
47. H. Takahashi, Y. Saito and M. Nagayama, *Kinzoku Hyomen Gijutsu*, **33**, 225 (1982).
48. J. W. Diggie, T. C. Downie and C. W. Goulding, *Chem. Rev.*, 365 (1969).
49. J. J. Randall, Jr. and W. J. Bernard, *Electrochim. Acta*, **20**, 653 (1975).
50. W. J. Bernard, *J. Electrochem. Soc.*, **109**, 1082 (1962).
51. M. F. Abd Rabbo, J. A. Richardson and G. C. Wood, *Corros. Sci.*, **16**, 689 (1976).
52. S. Matsuzawa, N. Baba and S. Tajima, *Electrochim. Acta*, **24**, 1199 (1979).
53. H. Konno, S. Kobayashi, H. Takahashi and M. Nagayama, *Electrochim. Acta*, **25**, 1667 (1980).
54. K. Shimizu, G. E. Thompson and G. C. Wood, *Thin Solid Films*, **77**, 313 (1981).
55. G. E. Thompson, G. C. Wood and K. Shimizu, *Electrochim. Acta*, **26**, 951 (1981).
56. K. Shimizu, G. E. Thompson and G. C. Wood, *Thin Solid Films*, **81**, 39 (1981).
57. P. Skeldon, K. Shimizu, G. E. Thompson and G. C. Wood, *Surf. Interface Anal.*, **5**, 252 (1983).
58. D. L. Cocke, S. M. Kormali, C. V. Barros-Leite, O. J. Murphy, E. A. Schweikert, P. Filpus-Luyckx, C. A. Polansky and D. E. Halverson, *J. Chem. Soc. Chem. Commun.*, 1560 (1984).
59. H. Takahashi, K. Fujimoto, H. Konno and M. Nagayama, *J. Electrochem. Soc.*, **131**, 1856 (1984).
60. D. L. Cocke, C. A. Polansky, D. E. Halverson, S. M. Kormali, C. V. Barros-Leite, O. J. Murphy, E. A. Schweikert and P. Filpus-Luyckx, *J. Electrochem. Soc.*, **132**, 3065 (1985).
61. H. Takahashi, K. Fujimoto and M. Nagayama, *J. Electrochem. Soc.*, **135**, 1349 (1988).
62. W. J. Bernard and J. J. Randall, *J. Electrochem. Soc.*, **108**, 822 (1961).

63. R. C. McCune, *J. Vac. Sci. Technol.*, **15**, 31 (1978).
64. K. Matsuki, A. Sawaguchi and M. Sugawara, *Denki Kagaku*, **60**, 488 (1992).
65. H. Shimamoto, R. Hashimoto and H. Tokumasu, *Electrolytic Condenser Review*, **42**, 14 (1990).
66. S. Itami, *Electrolytic Condenser Review*, **44**, 114 (1993).
67. H. Steinberg, *Organoboron Chemistry*, Vol.1, Interscience, New York (1964).
68. S. D. Ross, R. C. Peterson and M. Finkelstein, *USP* 3,403,304 (1968).
69. R. W. Santway and R. S. Alwitt, *USP* 3,403,305 (1968).
70. S. D. Ross, F. S. Dunkl, *USP* 4,428,028 (1984).
71. M. P. Drake, *UK* 2,143,228A (1985).
72. H. Shimamoto, Y. Miyazaki, T. Tsunetsugu, H. Nagara, K. Mori, S. Yoshida, Y. Kuwae and K. Shiono, *JP* 88-169017A (1988).
73. M. Finkelstein, E. A. Mayeda and S. D. Ross, *J. Org. Chem.*, **40**, 804 (1975).
74. M. Ue, to be published.
75. J. G. Drawber and D. H. Matusin, *J. Chem. Soc. Faraday Trans. 1*, **78**, 2521 (1982).
76. H. Corti, R. Crovetto and R. Fernández-Prini, *J. Solution Chem.*, **9**, 617 (1980).
77. H. R. Rogers and C. M. G. van den Berg, *Talanta*, **35**, 271 (1988).
78. L. J. Csetenyi, F. P. Glasswe and R. A. Howie, *Acta Cryst.*, **C49**, 1039 (1993).
79. C. G. Salentine, *Inorg. Chem.*, **22**, 3920 (1983).
80. E. Bessler and J. Weidlein, *Z. Naturforsch.*, **37b**, 1020 (1982).
81. J. A. Dean, Editor, *Lange's Handbook of Chemistry*, 13th ed., McGraw-Hill, New York (1985).
82. M. Ue, unpublished results.

3. Organic Electrolytes for Electrical Double Layer Capacitors

3.1 Introduction

The electrical double layer capacitor is an electrochemical energy storage device, in which electric charge is stored in the electrical double layer formed at the interface between a polarizable electrode and an electrolyte solution when dc voltage is applied as shown in Fig. 1.

Application of electrical double layer capacitance to a real capacitor was proposed by General Electric Co. in 1954 followed by Standard Oil, IBM and Western Electric Co. (Bell Laboratory). However, it was not until 1978 that Matsushita Electric Industrial Co. mass-produced this device successfully for the first time in the world [1]. This was because there had been no market need for this kind of device before the semiconductor caused technological innovation in electric industries.

An electrical double layer capacitor is composed of a pair of activated carbon electrodes with high surface area ($> 1000 \text{ m}^2 \text{ g}^{-1}$) and an organic liquid electrolyte. The electrical double layer capacitance on an activated carbon electrode is reported to be about $5 \mu\text{F cm}^{-2}$ [18], which results in 50 F g^{-1} . The attainable capacitance C of the real capacitor, which is dependent on the working voltage V , is around 1 F cm^{-3} , which is about a thousand times larger than that of an aluminum electrolytic capacitor. The appearance and construction of these capacitors are given in Fig. 2.

These capacitors have been widely used as memory backup devices in many electronic appliances [1 - 6] and recent interest has been stimulated by the prospective application to load levelers in electric vehicle propulsion systems, since "Ultra Capacitors" or "Power Capacitors" with large capacities have higher pulse power capability than conventional rechargeable batteries [4, 5, 7, 8].

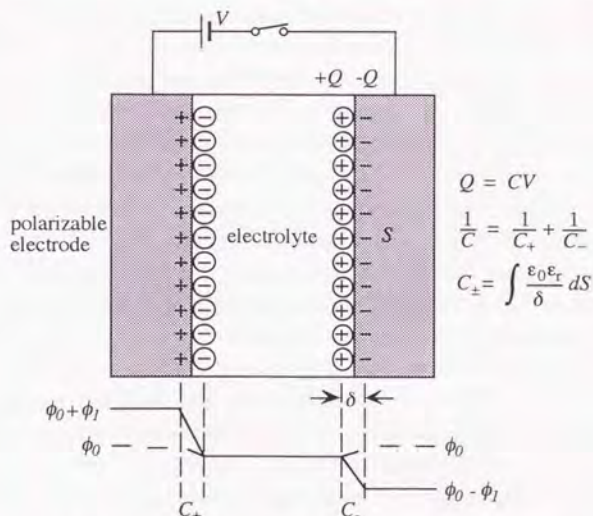


Fig. 1. Principle of electrical double layer capacitor.

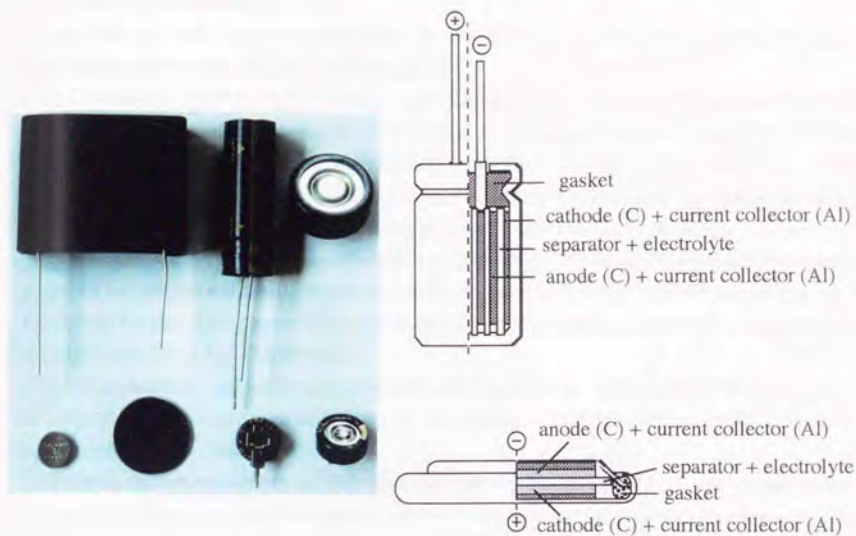


Fig. 2. Appearance and construction of electrical double layer capacitors.

The organic liquid electrolyte for these capacitors requires a high electrolytic conductivity and a high electrochemical stability over a wide temperature range and these requirements are more stringent than those for lithium batteries. Therefore, the selection of electrolyte materials is very restricted, for example, a popular electrolyte system comprising a lithium salt, a high permittivity solvent and a low viscosity solvent [9] cannot be used due to the low oxidation potential and low boiling point of the low viscosity solvent (See Chap. 4.2).

High permittivity solvents or their mixtures selected from propylene carbonate [10, 12, 14, 16 - 18], γ -butyrolactone [10, 11, 13, 15, 19], N, N-dimethylformamide [10, 13, 15], ethylene carbonate [19], sulfolane [15, 19, 20] and 3-methylsulfolane [20] have been examined by others.

In earlier research, alkali metal salts such as lithium perchlorate were examined as solutes in liquid electrolyte [10 - 13], however, onium salts such as tetraalkylammonium [14 - 16, 19] or tetraalkylphosphonium salts [17, 18, 20] have come into favor due to their better solubility and conductivity than the alkali metal salts in the high permittivity solvents.

Although tetraethylammonium tetrafluoroborate/propylene carbonate electrolyte (0.5 to 1 mol dm^{-3}) is the most common liquid electrolyte used in electrical double layer capacitors [5, 14, 16], we have examined the electrochemical properties of various organic liquid electrolytes based on quaternary onium salts to gain a better understanding and find better electrolytes for electrical double layer capacitors.

3.2. Preparation of Electrolyte Salts

Quaternary onium salts were prepared by the four methods depicted in Fig. 3, where reaction schemes are written for a tetraalkyl ammonium salt.

1) Tetramethyl-, tetraethyl-, tetrapropyl- and tetrabutylammonium salts were prepared by the titration of perchloric acid (Wako Pure Chemical Industries), tetrafluoroboric acid (Morita Chemical Industries), hexafluorophosphoric acid (Morita Chemical Industries) and trifluoromethanesulfonic acid (Tokyo Chemical Industry Co.) with the corresponding tetraalkylammonium hydroxide aqueous solutions (SACHEM Inc.). <Method A>

2) Ethyltrimethyl-, diethyldimethyl- and triethylmethylammonium tetrafluoroborates were prepared by the neutralization of tetrafluoroboric acid with the corresponding quaternary ammonium bicarbonate aqueous solutions obtained from the reaction of appropriate amines with dimethyl carbonate [21]. <Method B>

3) Tributylmethyl- and tetrahexylammonium tetrafluoroborates were prepared by the reaction of tributylmethylammonium iodide [22] and tetrahexylammonium bromide [22] with tetrafluoroboric acid [23]. <Method C>

4) Cyclic quaternary ammonium tetrafluoroborates were synthesized from the corresponding cyclic quaternary ammonium bromides or iodides by oxidative anion exchange in the presence of hydrogen peroxide and tetrafluoroboric acid [24, 25]. Cyclic quaternary ammonium bromides were prepared by a similar method described in the literature [26, 27]. <Method D>

5) Tetramethyl-, tetraethyl-, tetrapropyl- and tetrabutylphosphonium tetrafluoroborates were prepared by the treatment of the corresponding tetraalkylphosphonium bromides (Tokyo Chemical Industry Co.) with tetrafluoroboric acid. <Method C>

Most salts were purified by repeated recrystallization from isopropanol or acetone. Salts with a larger cation than tetraethylammonium or phosphonium were purified by redeposition into water from methanol or acetone solutions [28]. All the salts were vacuum dried at 100°C.

Method C always gives impure products contaminated by appreciable amounts of halide (several tens ppm), which caused fatal deterioration of the electrical double layer capacitor, and needs repeated recrystallization to purify. Method D was newly developed to circumvent this problem. This new process afforded a very pure salt, whose halide content is less than 1 ppm. This is because X_2 (Br_2 or I_2) is easier than HX (HBr or HI) to remove from the reaction mixture. It was found that this method is particularly useful for asymmetric bromides, because liquid polybromides called "Bromine Oil" are formed during the reaction, which are susceptible to bromine liberation.

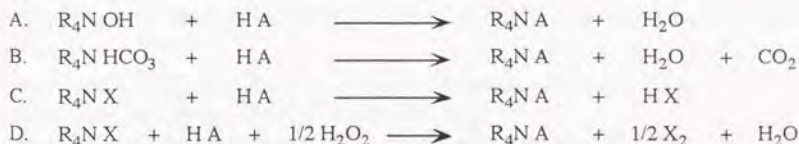


Fig. 3. Preparation methods of quaternary ammonium salts.

3.2.1. Experimental

Among synthesized quaternary ammonium salts, N-ethyl-N-methyl-substituted alicyclic ammonium tetrafluoroborates are new compounds. For more details, refer to author's patents [24, 29].

1-ethyl-1-methylpyrrolidinium tetrafluoroborate

513.9 g (2.65 mol) of 1-ethyl-1-methylpyrrolidinium bromide was dissolved in 598.7 g (2.86 mol) of 42 wt% tetrafluoroboric acid aqueous solution. 154.4 g (1.59 mol) of 35 wt% hydrogen peroxide aqueous solution was added dropwise at room temperature. The resulting bromine was removed from the reaction mixture by evaporation under reduced pressure (20 mm Hg) at 40°C. When the mixture became homogeneous, 100 g of water was added and evaporation was continued. The resultant slurry was recrystallized from 1180 g of isopropanol to give 516.8 g of a white crystalline. The yield was 97.1 %. mp: 287°C.

Elemental analysis: Calcd. for $C_7H_{16}NBF_4$: C, 41.83; H, 8.02; N, 6.97. Found: C, 41.88; H, 8.26; N, 6.91.

1H -n.m.r. (in DMSO- d_6) in ppm relative to TMS: 1.27 (3H, t, $-CH_2-CH_3$), 1.73 - 2.20 (4H, m, $-CH_2-CH_2-$), 2.97 (3H, s, N- CH_3), 3.20 - 3.56 (6H, m, N- CH_2-).

ir (KBr) in cm^{-1} : 3430, 2950, 1460, 1300, 1020, 540, 520

1-ethyl-1-methylpiperidinium tetrafluoroborate

50.0 g (0.2 mol) of 1-ethyl-1-methylpiperidinium iodide was dissolved in 45.1 g (0.22 mol) of 42 wt% tetrafluoroboric acid aqueous solution. 10.7 g (0.11 mol) of 35 wt% hydrogen peroxide aqueous solution was added dropwise at room temperature. The upper layer was separated and evaporated to dryness. The product was recrystallized from 60 g of methanol to give 29.0 g of a white crystalline. The yield was 66.7 %. mp: 274°C.

Elemental analysis: Calcd. for $C_8H_{18}NBF_4$: C, 44.68; H, 8.44; N, 6.51. Found: C, 44.95; H, 8.71; N, 6.47.

1H -n.m.r. (in DMSO- d_6) in ppm relative to TMS: 1.23 (3H, t, $-CH_2-CH_3$), 1.40 - 2.00 (6H, m, $-CH_2-CH_2-$), 2.97 (3H, s, N- CH_3), 3.13 - 3.57 (6H, m, N- CH_2-).

ir (KBr) in cm^{-1} : 3430, 2950, 1620, 1470, 1300, 1020, 540, 520

1-ethyl-1-methylmorpholinium tetrafluoroborate

30.0 g (0.12 mol) of 1-ethyl-1-methylmorpholinium iodide was dissolved in 29.3 g (0.14 mol) of 42 wt% tetrafluoroboric acid aqueous solution. 6.6 g (0.07 mol) of 35 wt% hydrogen peroxide aqueous solution was added dropwise at room temperature. The upper layer was separated and evaporated to dryness. The product was recrystallized from 30 g of methanol to give 21.8 g of a white crystalline. The yield was 86.2 %. mp: 158°C.

Elemental analysis: Calcd. for $C_7H_{16}NOBF_4$: C, 38.74; H, 6.45; N, 7.43. Found: C, 38.51; H, 6.30; N, 6.99.

1H -n.m.r. (in DMSO- d_6) in ppm relative to TMS: 1.34 (3H, t, $-CH_2-CH_3$), 3.16 (3H, s, N- CH_3), 3.34 - 3.67 (6H, m, N- CH_2-), 3.84 - 4.10 (4H, m, O- CH_2-).

ir (KBr) in cm^{-1} : 3400, 2990, 2280, 1640, 1460, 1120, 890, 540, 520

3.3. Electrochemical Properties of Organic Electrolytes

The electrolytic conductivity and stable potential window of an organic liquid electrolyte are important electrochemical properties. The electrolytic conductivity directly affects the internal resistance of a capacitor, which leads to energy loss during charge-discharge cycling. The stable potential window determines the maximum operational voltage of a capacitor, which manages total charge by CV product. These electrochemical properties of organic liquid electrolytes are discussed from the chemical structures of three components; cation, anion and solvent.

3.3.1. Experimental

Electrolyte preparation

Propylene carbonate, butylene carbonate and γ -butyrolactone (Mitsubishi Petrochemical Co., Battery-grade F-PC, F-BC and F-GBL) were used without further purification. All other solvents (Tokyo Chemical Industry Co.) were purified by careful distillation over molecular sieve 5A, which resulted in more than 99.8 % purity detected by a capillary gas chromatography. An electrolyte salt was dissolved in a purified solvent and the resulting electrolyte was vacuum dried at 50°C until water content dropped less than 100 ppm.

Measurements

The relative permittivity and viscosity of solvents were measured by an LCR meter equipped with a capacitor cell (Ando Electric Co., AG-4311), and a viscosity meter (Tokyo Keiki Co., Visconic ED), respectively.

The electrolytic conductivity and water content of electrolytes were measured by a conductivity meter equipped with a standard type conductivity cell (Toa Electronics, CM-60S/CGT-511B) and a moisture meter (Mitsubishi Kasei Co., CA-06), respectively.

The limiting reduction and oxidation potentials were measured by linear sweep voltammetry with an automatic polarization system (Hokuto Denko Co., HZ-1A). A pair of 3 ϕ glassy carbon rods (Tokai Carbon Co., GC-10) were used as working and counter electrodes. The sidewall of the working electrode was sealed with a thermo-shrinkable tube to limit the surface area to 7 mm². The surface was polished with alumina powder before use. A saturated calomel electrode (Toa Electronics, HC-205C) was isolated *via* KCl-agar and electrolyte bridge. Measurement was carried out in a nitrogen atmosphere glove box using the cell assembly depicted in Fig. 4.

3.3.2. Results and Discussion

Selection of solute

Tetraalkylammonium salts have been widely used as a supporting electrolyte salt in nonaqueous solvents, because of their high solubility, electrolytic conductivity, electrochemical stability and ease of preparation and purification. However, systematic data such as the electrolytic conductivity at practical concentrations are surprisingly scarce and fragmented data are scattered in the literature [23, 30, 31].

The electrolytic conductivities σ of lithium and symmetric tetraalkylammonium salts with popular anions were measured in propylene carbonate (PC) and γ -butyrolactone (GBL) at 1 mol dm⁻³ and 25°C. The results are given in Table 1, together with values in N, N-dimethylformamide (DMF) and acetonitrile (AN), which are mostly cited from the literature [23, 30].

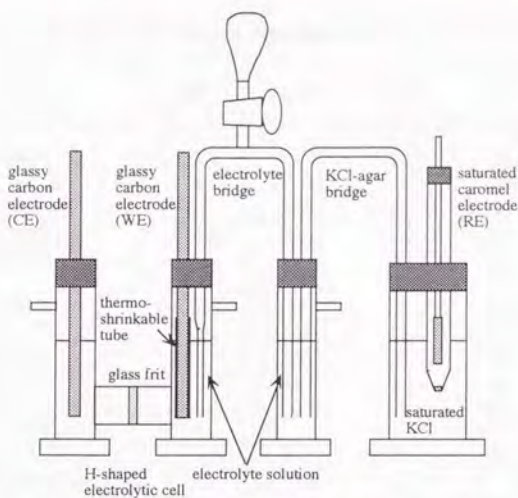
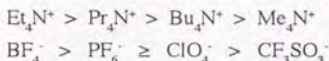


Fig. 4. Schematic diagram of cell assembly used in polarization experiments.

The conductivities generally decrease in the following order:



Tetramethylammonium salts were not useful except for trifluoromethanesulfonate due to their low solubilities. Tetraethylammonium salts are most favorable in conductivity. The highest conductivity of tetraethylammonium tetrafluoroborate appears to come from the small anion size and moderate dissociation tendency.

The stable potential window is defined as a potential region where no appreciable faradaic current flows. Different criteria have been used for the evaluation of limiting reduction and oxidation potentials (E_{red} and E_{ox}) by different researchers. These values depend on the concentration and the purity of a liquid electrolyte. Even though the same electrode and electrolyte are used, these values are also dependent on current density and potential scan rate. For example, as to the current density, 0.01 [32], 0.1 [33], 0.2 [34], 0.5 [19, 35], 1 [36, 37], 1.5 [38] and 3 mA cm^{-2} [39] were adopted by others. The scan rate ranged from 2 to 100 mV s^{-1} for these values [32, 33, 35, 37 - 39].

The limiting reduction and oxidation potentials were defined here as the potentials at which the current density exceeded 1 mA cm^{-2} when the supporting electrolyte concentration was 0.65 mol dm^{-3} [40] and the scan rate was 5 mV s^{-1} . A glassy carbon electrode was used as a working electrode because it is a better substitute for the activated carbon electrode than platinum or mercury electrodes.

Typical polarization curves are shown in Fig. 5, where the cathodic and anodic polarizations were carried out separately, and potential is reported relative to the saturated calomel electrode

Table 1. Electrolytic conductivities of organic electrolytes at 1 mol dm⁻³, 25°C.

| Electrolyte | PC | GBL | DMF | AN |
|---------------------------------------------------|-------|-------|-------------------|-------------------|
| Li BF ₄ | 3.4 | 7.5 | 22 | 18 |
| Me ₄ N BF ₄ | 2.7 * | 2.9 * | 7.0 * | 10 * |
| Et ₄ N BF ₄ | 13 | 18 | 26 ^a | 56 ^a |
| Pr ₄ N BF ₄ | 9.8 | 12 | 20 ^a | 43 ^a |
| Bu ₄ N BF ₄ | 7.4 | 9.4 | 14 ^a | 32 ^a |
| Li PF ₆ | 5.8 | 11 | 21 | 50 |
| Me ₄ N PF ₆ | 2.2 * | 3.7 * | 11 * | 12 * |
| Et ₄ N PF ₆ | 12 | 16 | 25 | 55 |
| Pr ₄ N PF ₆ | 6.4 * | 11 | 19 | 42 |
| Bu ₄ N PF ₆ | 6.1 | 8.6 | 13 | 31 |
| Li ClO ₄ | 5.6 | 11 | 20 | 32 |
| Me ₄ N ClO ₄ | 2.9 * | 3.9 * | 7.8 * | 7.7 * |
| Et ₄ N ClO ₄ | 11 | 16 | 24 ^a | 50 ^a |
| Pr ₄ N ClO ₄ | 6.3 * | 11 * | 17 * ^a | 35 * ^a |
| Bu ₄ N ClO ₄ | 6.0 | 8.1 | 12 ^a | 27 ^a |
| Li CF ₃ SO ₃ | 1.7 | 4.3 | 16 | 9.7 |
| Me ₄ N CF ₃ SO ₃ | 9.0 * | 14 | 24 | 46 |
| Et ₄ N CF ₃ SO ₃ | 11 | 15 | 21 ^b | 42 ^b |
| Pr ₄ N CF ₃ SO ₃ | 7.8 | 11 | 15 ^b | 31 ^b |
| Bu ₄ N CF ₃ SO ₃ | 5.7 | 7.4 | 11 ^b | 23 ^b |

in mS cm⁻¹, * saturated solution (< 1 mol dm⁻³).

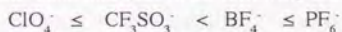
^a Ref. 23, ^b Ref. 30.

(SCE).

The limiting reduction and oxidation potentials for tetraethylammonium salts in propylene carbonate are summarized in Table 2.

The reduction potential appeared to be limited by the decomposition of both tetraethylammonium cation and propylene carbonate solvent because the reduction resulted in the formation of a polymer on the electrode and gas evolution, which contained carbon dioxide, propylene and triethylamine [41].

The oxidation potentials was limited by the decomposition of ClO₄⁻ and CF₃SO₃⁻ not by BF₄⁻ and PF₆⁻, which were more resistant to oxidation than propylene carbonate. The electrochemical stability of the anion increases in the following order [19, 36, 42]:



The decomposition of propylene carbonate can be one electron reduction in the carbon atom and one electron oxidation from the oxygen atom in C=O bond from frontier orbital calculations [43].

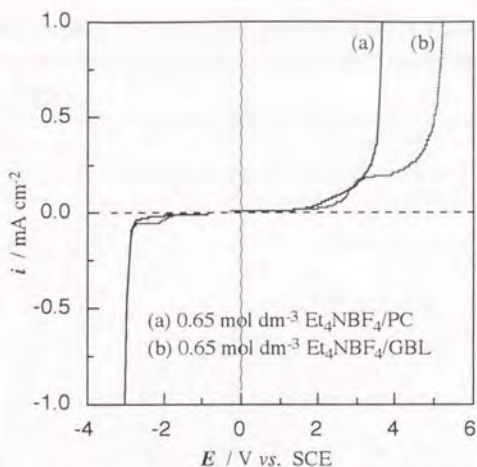


Fig. 5. Typical polarization curves of organic electrolytes on a glassy carbon electrode.

Table 2. Electrolytic conductivities, limiting reduction and oxidation potentials of PC electrolytes at 0.65 mol dm⁻³, 25°C.

| Electrolyte | σ / mS cm ⁻¹ | E_{red} / V vs. SCE | E_{ox} |
|---------------------------------------------------|-----------------------------------|---------------------------------|-----------------|
| Et ₄ N BF ₄ | 10.55 | - 3.0 | + 3.6 |
| Et ₄ N PF ₆ | 9.64 | - 3.0 | + 3.6 |
| Et ₄ N ClO ₄ | 9.94 | - 3.0 | + 3.1 |
| Et ₄ N CF ₃ SO ₃ | 9.38 | - 3.0 | + 3.1 |

Selection of solvent

Dipolar aprotic solvents, which exhibit no appreciable tendency to participate in the transfer of protons but are moderately good solvating and ionizing media due to their dipolar nature and their high relative permittivity more than 20 [44], are essential for the liquid electrolyte of electrical double layer capacitors to gain a large enough stable potential window. Twenty dipolar aprotic solvents have been selected, whose melting point (mp) and boiling point (bp) are below 30°C and over 100°C (except AN), respectively. These include not only popular solvents such as carbonate, lactone, nitrile, amide, nitro, sulfone, sulfoxide and phosphate [45, 46], but also uncommon difunctional solvents such as dinitrile and ethernitrile. Two homologues were selected in each category, if possible, as shown in Table 3, where physical properties of these solvents are listed.

Since Et₄N BF₄ showed the highest conductivity and BF₄⁻ is more stable to hydrolysis than PF₆⁻

Table 3. Physical properties of dipolar aprotic solvents and electrolytic conductivities, limiting reduction and oxidation potentials of their organic electrolytes containing 0.65 mol dm⁻³ Et₄NBF₄ at 25°C.

| Solvent | ϵ_r | η / cp | bp / °C | mp / °C | MW | σ / mS cm ⁻¹ | E _{red} / V vs. SCE | E _{ox} / V vs. SCE |
|---------------------------------------|-----------------|-------------------|------------------|------------------|-----|-----------------------------------|---------------------------------|--------------------------------|
| Propylene carbonate (PC) | 65 | 2.5 | 242 | -49 | 102 | 10.6 | -3.0 | +3.6 |
| Butylene carbonate (BC) | 53 ^a | 3.2 ^a | 240 ^a | -53 ^a | 116 | 7.5 | -3.0 | +4.2 |
| γ -Butyrolactone (GBL) | 42 | 1.7 | 204 | -44 | 86 | 14.3 | -3.0 | +5.2 |
| γ -Valerolactone (GVL) | 34 ^a | 2.0 ^a | 208 ^b | -31 ^b | 100 | 10.3 | -3.0 | +5.2 |
| Acetonitrile (AN) | 36 | 0.3 | 82 | -49 | 41 | 49.6 | -2.8 | +3.3 |
| Propionitrile (PN) | 26 ^a | 0.5 ^a | 97 | -93 | 55 | insoluble | | |
| Glutaronitrile (GLN) | 37 ^a | 5.3 ^a | 286 ^b | -29 ^b | 94 | 5.7 | -2.8 | +5.0 |
| Adiponitrile (ADN) | 30 ^a | 6.0 ^a | 295 ^b | 2 ^b | 108 | 4.3 | -2.9 | +5.2 |
| Methoxyacetonitrile (MAN) | 21 ^a | 0.7 ^a | 120 ^b | -35 ^a | 71 | 21.3 | -2.7 | +3.0 |
| 3-Methoxypropionitrile (MPN) | 36 ^a | 1.1 ^a | 165 ^b | -57 ^a | 85 | 15.8 | -2.7 | +3.1 |
| N,N-Dimethylformamide (DMF) | 37 | 0.8 | 153 | -61 | 73 | 22.8 | -3.0 | +1.6 |
| N,N-Dimethylacetamide (DMA) | 38 | 0.9 | 166 | -20 | 87 | 15.7 | | |
| N-Methylpyrrolidinone (NMP) | 32 | 1.7 | 202 | -24 | 99 | 8.9 | | |
| N-Methyloxazolidinone (NMO) | 78 ^c | 2.5 ^c | 270 ^b | 15 ^b | 101 | 10.7 | -3.0 | +1.7 |
| N,N'-Dimethylimidazolidinone (DMI) | 38 ^d | 1.9 ^d | 226 ^d | 8 ^d | 114 | 7.0 | -3.0 | +1.2 |
| Nitromethane (NM) | 38 | 0.6 | 101 | -29 | 61 | 33.8 | -1.2 | +2.7 |
| Nitroethane (NE) | 28 ^a | 0.7 ^a | 115 ^b | -90 ^b | 75 | 22.1 | -1.3 | +3.2 |
| Sulfolane (TMS) | 43 | 10.0 (30°C) | 287 | 28 | 120 | 2.9 | -3.1 | +3.3 |
| 3-Methylsulfolane (3MS) | 29 ^e | 11.7 ^e | 276 ^b | 6 ^b | 134 | insoluble | | |
| Dimethylsulfoxide (DMSO) | 47 | 2.0 | 189 | 19 | 78 | 13.9 | -2.9 | +1.5 |
| Trimethyl phosphate (TMP) | 21 ^a | 2.2 ^a | 197 ^b | -46 ^b | 140 | 8.1 | -2.9 | +3.5 |

Physical properties are cited from Ref. 45 and 46 except ^a our data, ^b Ref. 48, ^c Ref. 32, ^d Ref. 49 and ^e Ref. 50.

[47], we have adopted $\text{Et}_4\text{N BF}_4$ as the supporting electrolyte salt for examining solvents. Electrolytic conductivities and limiting reduction and oxidation potentials of the liquid electrolytes containing $0.65 \text{ mol dm}^{-3} \text{ Et}_4\text{N BF}_4$ are given in Table 3.

Many solvents with lower viscosities than propylene carbonate showed higher conductivity of electrolytes. The observed electrolytic conductivities of the electrolytes were plotted against the reciprocals of the solvent viscosities η and a good linear relationship was obtained as shown in Fig. 6 (correlation coefficient $\gamma = 0.97$). On the other hand, no correlation between the electrolytic conductivity of the electrolyte and the relative permittivity ϵ_r of the solvent was observed as shown in Fig. 7. These results indicate that $\text{Et}_4\text{N BF}_4$ is almost equally dissociated in any higher permittivity solvent ($\epsilon_r > 20$), and conductivity is only dependent on ionic mobility. Therefore, Walden law is realized in these concentrated solutions.

We have found a close relationship between the electrolytic conductivity of the electrolyte and the reciprocal of molecular weight MW of the solvent as shown in Fig. 8 ($\gamma = 0.96$). This observation suggests the existence of some solvent-solute interaction, although ion-solvent interaction can be neglected at infinite dilution (See Chap. 3.4). Because ionic mobility depends on the formula weight FW of the ion (See Chap. 3.4), which apparently can be increased by the solvation.

Although there is no quantitative information on solvent-solute interaction, the molecular weight of the solvent can act as a good parameter to estimate the electrolytic conductivity in onium salt/dipolar aprotic solvent systems. For example, propylene carbonate, γ -valerolactone and N-methyloxazolidinone having similar cyclic structures and molecular weight showed almost the

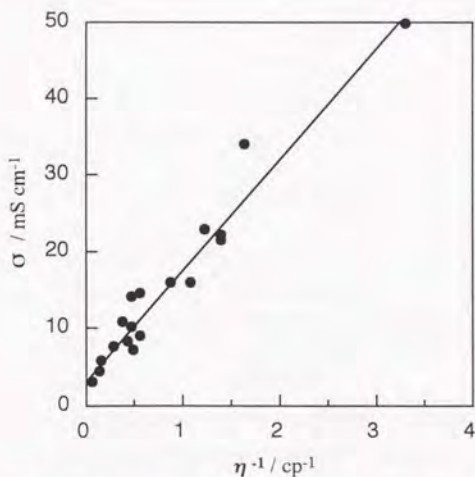


Fig. 6. Relationship between electrolyte conductivity and reciprocal of the solvent viscosity.

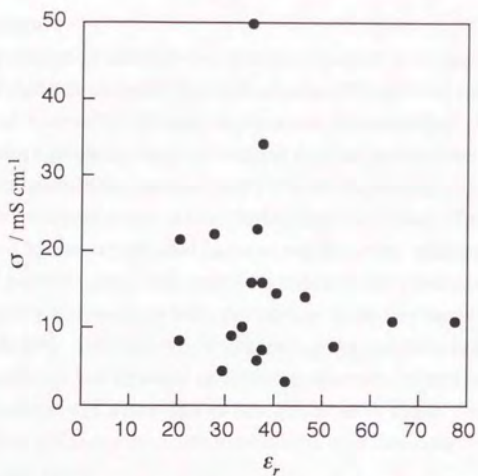


Fig. 7. Relationship between electrolyte conductivity and relative permittivity of the solvent .

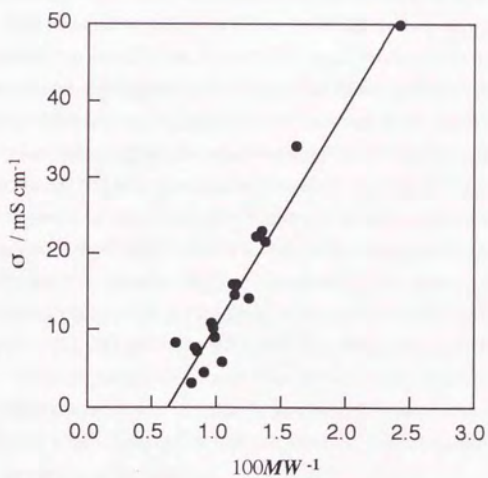


Fig. 8. Relationship between electrolyte conductivity and reciprocal of molecular weight of the solvent.

same electrolytic conductivity.

Direct comparison of limiting reduction and oxidation potentials is not precise. In principle, this is because the liquid junction potential between an organic liquid electrolyte and an aqueous saturated KCl solution is varied by the kind of organic liquid electrolyte. However, the values obtained are useful from a practical viewpoint because they are reproducible within about 0.1 V.

Most solvents except nitroalkanes showed a similar reduction potential (-3.0 V vs. SCE), which may be limited by the decomposition of tetraethylammonium cation. The limiting oxidation potential was extended by the utilization of lactones and dinitriles. Although the more positive oxidation potential of γ -butyrolactone than propylene carbonate has already been known [10, 38], the oxidation potential of γ -valerolactone was reported to be lower than that of propylene carbonate on a platinum electrode [38]. The durability of dinitriles against oxidation is first demonstrated, to our knowledge. The solvents having amide or sulfoxide structures showed much lower oxidation potentials due to the existence of a lone-pair on nitrogen or sulfur atom. This is the main reason why these solvents have not been used in electrical double layer capacitors.

Effect of contaminated water

The main factor producing ambiguity in some properties of dipolar aprotic solvents is contamination by water because a trace amount of amphiprotic solvents substantially alters the nature of the electrode process in aprotic solvent systems.

During the polarization experiments, a narrower potential window, particularly, a lower oxidation potential was observed, when water contamination exceeded around 300 ppm. To avoid water contamination from an aqueous reference electrode (SCE), a silver wire was often used to get reliable values. Although the equilibrium potential of Ag/Ag^+ (dissolved anodically) shifted in some cases, almost the same stable potential window and lower residual current were observed when the SCE reference electrode was replaced with a silver wire as shown in Fig. 9. Utilization of this simple reference electrode enabled the measurements at elevated temperatures as shown in Fig. 10. The stable potential window shrank as temperature increased. Such measurement at an elevated temperature is useful to understand the behavior of actual capacitor cells.

Current increase caused by hydrolysis of both solvent and solute was confirmed by polarization experiments, where the addition of water was correlated with hydrolysis products. For example, hydrolysis products such as propylene glycol from propylene carbonate [51], γ -hydroxybutyric acid from γ -butyrolactone [52, 53] and $\text{HF} + \text{BF}_3(\text{OH})^-$ from BF_4^- [54] were detected.

γ -Butyrolactone is the most promising solvent from the viewpoint of electrolytic conductivity and a stable potential window as shown in Table 3, however, it is more susceptible to hydrolysis than propylene carbonate, which hindered its intrinsic electrochemical stability.

Optimization of quaternary onium cation

The effect of cation structure of quaternary onium tetrafluoroborate salts on the electrochemical properties of their propylene carbonate electrolytes was examined. The electrolytic conductivities and limiting reduction and oxidation potentials of organic liquid electrolytes consisting of many kinds of quaternary ammonium or phosphonium tetrafluoroborate and propylene carbonate are given in Table 4.

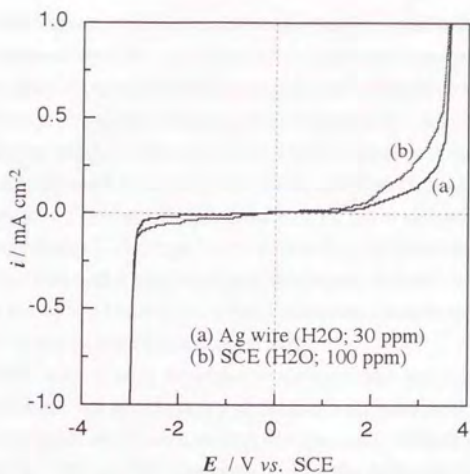


Fig. 9. Effect of contaminated water on electrochemical potential window of $0.65 \text{ mol dm}^{-3} \text{ Et}_4\text{NBF}_4/\text{PC}$ electrolyte.

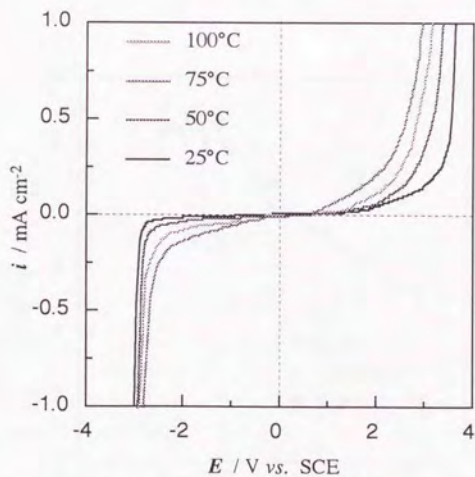


Fig. 10. Effect of temperature on electrochemical potential window of $0.65 \text{ mol dm}^{-3} \text{ Et}_4\text{NBF}_4/\text{PC}$ electrolyte.

Previously, we have reported that the maximum electrolytic conductivity of organic liquid electrolytes at practical concentrations was observed for asymmetric quaternary ammonium salts having sizes between those of tetramethylammonium and tetraethylammonium salts (See Chap. 2.4). This observation was confirmed further by the introduction of cyclic quaternary ammonium salts in this work. Higher conductivities were obtained for quaternary ammonium salts having formula weights between those of tetramethylammonium and tetraethylammonium salts as shown in Fig. 11. Quaternary phosphonium salts showed a little bit lower electrolytic conductivity than corresponding ammonium salts [17] except for the tetramethylphosphonium salt, which has much better solubility than the tetramethylammonium salt, presumably because of a larger atomic radius for phosphorous than nitrogen. However, quaternary phosphonium salts appear to show the same conductivity behavior as the quaternary ammonium salts.

To understand the reason why asymmetric quaternary ammonium salts such as triethylmethylammonium, ethylmethylpyrrolidinium and tetramethylenepyrrolidinium tetrafluoroborates have higher conductivities than the symmetric tetraethylammonium salt, the degree of dissociation at 0.65 mol dm^{-3} was calculated by the Arrhenius equation, $\alpha = \Lambda / \Lambda_0$, where α , Λ and Λ_0 are the degree of dissociation, molar conductivity and limiting molar conductivity, respectively. The results are given in Table 5, where the limiting molar conductivities of acyclic quaternary ammonium salts are experimental values and those for cyclic quaternary ammonium salts are estimated values (See Chap. 3.4).

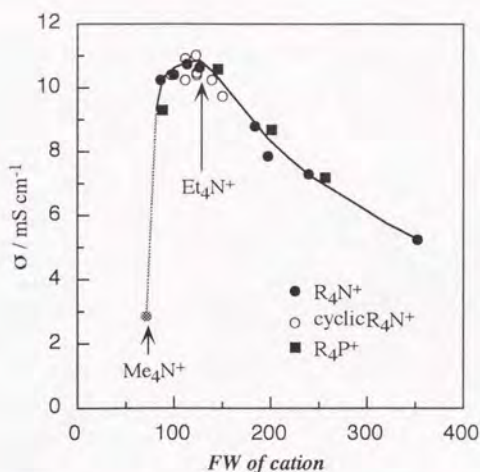
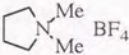
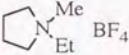
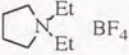
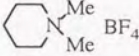
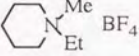
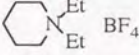
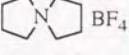
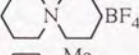
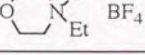


Fig. 11. Relationship between electrolytic conductivity and formula weight of quaternary ammonium and phosphonium cation.

Table 4. Electrolytic conductivities, limiting reduction and oxidation potentials of PC electrolytes containing 0.65 mol dm⁻³ quaternary ammonium or phosphonium tetrafluoroborate at 25°C.

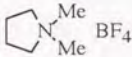
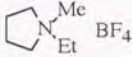
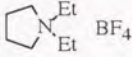
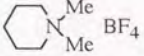
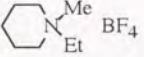
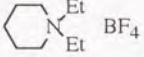
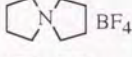
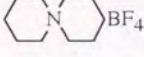
| Electrolyte | σ / mS cm ⁻¹ | E_{red} / V vs. SCE | E_{ox} |
|-----------------------------------------------------------------------------------------------------|-----------------------------------|---------------------------------|-----------------|
| Me ₄ N BF ₄ (0.1 mol dm ⁻³) | 2.41 | -3.10 | +3.50 |
| Me ₃ EtN BF ₄ | 10.16 | -3.00 | +3.60 |
| Me ₂ Et ₂ N BF ₄ | 10.34 | -3.00 | +3.65 |
| MeEt ₃ N BF ₄ | 10.68 | -3.00 | +3.65 |
| Et ₄ N BF ₄ | 10.55 | -3.00 | +3.65 |
| Pr ₄ N BF ₄ | 8.72 | -3.05 | +3.65 |
| MeBu ₃ N BF ₄ | 7.80 | | |
| Bu ₄ N BF ₄ | 7.23 | -3.05 | +3.65 |
| Hex ₄ N BF ₄ | 5.17 | -3.10 | +3.85 |
| Me ₄ P BF ₄ | 9.21 | -3.05 | +3.60 |
| Et ₄ P BF ₄ | 10.52 | -3.00 | +3.60 |
| Pr ₄ P BF ₄ | 8.63 | -3.05 | +3.60 |
| Bu ₄ P BF ₄ | 7.14 | -3.05 | +3.80 |
|  BF ₄ | 10.36 | -3.00 | +3.65 |
|  BF ₄ | 10.82 | -3.00 | +3.70 |
|  BF ₄ | 10.40 | -3.00 | +3.60 |
|  BF ₄ | 10.20 | -3.05 | +3.65 |
|  BF ₄ | 10.40 | -3.05 | +3.70 |
|  BF ₄ | 10.17 | -3.05 | +3.60 |
|  BF ₄ | 10.94 | -3.00 | +3.60 |
|  BF ₄ | 9.67 | -3.00 | +3.60 |
|  BF ₄ | 8.78 | -3.00 | +3.60 |

Triethylmethylammonium, ethylmethylpyrrolidinium and tetramethylenepyrrolidinium tetrafluoroborates have almost the same degree of dissociation as the tetraethylammonium salt. We conclude that the higher conductivities of these three salts come from their smaller ion sizes without losing their high dissociation nature even at the practical concentration of 0.65 mol dm^{-3} .

These results have encouraged us to examine the electrolytic conductivity for more concentrated solutions, and we have found these three salts increase their conductivities until about 2 mol dm^{-3} due to their high solubility in propylene carbonate, whereas the tetraethylammonium counterpart can be dissolved up to only 1 mol dm^{-3} as shown in Fig. 12.

All quaternary ammonium and phosphonium tetrafluoroborates showed similar limiting reduction and oxidation potentials as shown in Table 4. No remarkable negative potential shift for limiting reduction potentials with increasing cation size was observed as was observed on mercury electrodes [23, 34, 37].

Table 5. Calculated molar conductivities, limiting molar conductivities and degree of dissociation.

| Electrolyte | Λ / $\text{S cm}^2 \text{ mol}^{-1}$ | Λ_0 | α |
|---------------------------------------------------------------------------------------------------|-------------------------------------------------|-------------|----------|
| $\text{Me}_4\text{N BF}_4$ (0.1 mol dm^{-3}) | 24.10 | 35.0 | 0.69 |
| $\text{Me}_3\text{EtN BF}_4$ | 15.63 | 34.9 | 0.45 |
| $\text{Me}_2\text{Et}_2\text{N BF}_4$ | 15.91 | 34.6 | 0.46 |
| $\text{MeEt}_3\text{N BF}_4$ | 16.43 | 34.3 | 0.48 |
| $\text{Et}_4\text{N BF}_4$ | 16.23 | 33.8 | 0.48 |
|  BF_4 | 15.94 | 34.4 | 0.46 |
|  BF_4 | 16.65 | 34.2 | 0.49 |
|  BF_4 | 16.00 | 34.0 | 0.47 |
|  BF_4 | 15.69 | 34.2 | 0.46 |
|  BF_4 | 16.00 | 34.0 | 0.47 |
|  BF_4 | 15.65 | 33.8 | 0.46 |
|  BF_4 | 16.83 | 34.0 | 0.50 |
|  BF_4 | 14.88 | 33.6 | 0.44 |

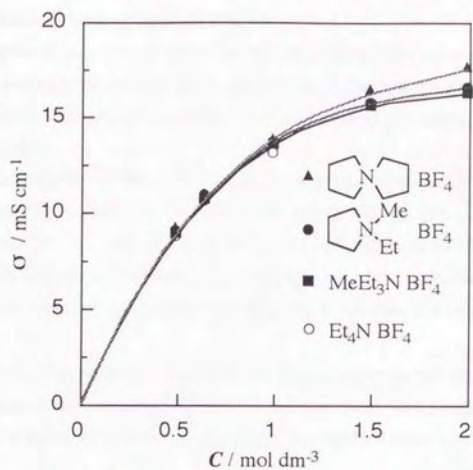


Fig. 12. Concentration dependence of electrolytic conductivities of several quaternary ammonium tetrafluoroborates in PC at 25°C.